# Collective Fluctuations in Ordered Fluids Investigated by Two-Dimensional Electron−Electron Double Resonance Spectroscopy

**Barbara Fresch,[†] Diego Frezzato,[†] Giorgio J. Moro,*[,†] Gerd Kothe,[‡] and Jack H. Freed[§]**

*Department of Chemical Science, University of Padova, Via Loredan 4, 35131 Padova, Italy, Department of Physical Chemistry, University of Freiburg, Albertstrasse 21, D-79104 Freiburg, Germany, and Baker Laboratory of Chemistry, Cornell University, Ithaca, New York 14853*

*Received: June 27, 2006; In Final Form: September 8, 2006*

Two-dimensional electron−electron double resonance (2D-ELDOR) is a technique that is sensitive to the dynamical processes affecting spin labels in complex fluid environments. In ordered fluids, such as membrane vesicles, the 2D-ELDOR experiment is affected by the molecular tumbling in the locally ordered environment. This motion occurs on two different time scales, the faster molecular motion relative to the local director, and the slower collective fluctuations of the director field. In the experimental study of Patyal, Crepeau, and Freed (*Biophys. J.* **1997**, *73*, 2201), it was found that the widths of the autopeaks of the 2D-ELDOR spectrum increased as a function of the mixing time. In the present work, a theory is developed for the effects of director fluctuations on the autopeaks in the 2D-ELDOR experiment by employing an analytical solution of the stochastic Liouville equation for which the director field is treated as a multidimensional Gaussian process, as previously developed by Frezzato, Kothe, and Moro (*J. Phys. Chem. B* **2001**, *105*, 1281 and *J. Phys. Chem. B* **2004**, *108*, 9505). Good agreement is found between theory and experiment, notably the only adjustable parameter is $\kappa$, the bending elastic modulus of the membrane. The values of $\kappa = 11 \times 10^{-20}$ J for 1,2-dipalmitoyl-*sn*-glycero-phosphatidylcholine (DPPC) vesicles and $\kappa = 15 \times 10^{-20}$ J for DPPC/gramicidin A (5:1) vesicles, both at 45 °C, were found from the analysis and agree well with previous related measurements by other physical techniques. This establishes 2D-ELDOR as a useful technique to study the elastic properties of biological membranes.

## 1. Introduction

Electron spin resonance (ESR) is a versatile spectroscopic technique that provides a wealth of information on the molecular structure of various paramagnetic systems. In addition, it can be used to characterize the dynamics of spin probes embedded in diamagnetic systems provided that the rotational motions modulate the magnetic interactions. This application, however, requires suitable theoretical tools for interpreting the effects of the molecular motions on the spectroscopic observables. The simplest situation is certainly that of a fast tumbling spin probe in an isotropic liquid, where the spectral line widths can be analyzed according to motional narrowing theory[1,2] based on a separate treatment of the reorientational motions and the dynamics of the spin degrees of freedom. A quite different approach is required in the absence of a time scale separation between the magnetic anisotropies (in frequency units) and the reorientational rates. In this case, a *slow motion theory* has to be employed involving a solution of the stochastic Liouville equation (SLE),[3−6] which describes the coupled evolution of the spin degrees of freedom and the stochastic variables for the probe orientation. This ensures a rather general treatment of the magnetization dynamics, albeit analytical solutions for the direct interpretation of experimental observables are not available. The standard solution procedure is based on a matrix representation of the SLE evolution operator to be generated by using a suitable basis for both the spin degrees of freedom and the functional dependence on the stochastic variables.[7] An algebraic solution can then be achieved by employing efficient algorithms to diagonalize this matrix.[8]

A more complex situation arises for spin probes dissolved in ordered fluids such as liquid crystals and biological membranes or their model systems such as vesicles. In these systems, the spin probe senses an orientational potential with respect to the local director determining the axis of the most probable molecular orientation. The director, which depends on the location within the sample and therefore should be represented by a vector field, has an intrinsic collective character and its fluctuations are controlled by the viscous and elastic properties of the ordered phase.[9−11] Thus, two completely different dynamical processes have to be considered in the analysis of the experimental observables: (i) the molecular tumbling with respect to the local director and (ii) the fluctuations of the director field. While the molecular tumbling occurs on well-defined time scales (often in the fast motion range), the fluctuations of the director are characterized by a wide distribution of relaxation times with components in the millisecond range or even slower.[9−11]

We shall consider the specific case (and perhaps the most interesting one from the point of view of studying director fluctuations[12]) of a spin probe embedded in an oriented fluid whose molecular motions occur within the fast motion regime. In that case, the motional narrowing theory[1,2] can be employed to describe the magnetic relaxation effects of the rotational tumbling with respect to the local director. Clearly, the same approach is inadequate for the modeling of director fluctuations

* Corresponding author. E-mail: giorgio.moro@unipd.it.
[†] University of Padova.
[‡] University of Freiburg.
[§] Cornell University.

10.1021/jp064028u CCC: $33.50 
Published on Web 11/09/2006

because these collective modes involve slow-motional components whose frequencies are much smaller than the magnetic anisotropies (in frequency units). Under these conditions, it is necessary to employ the full treatment according to the SLE for the dynamical coupling between the spin degrees of freedom and the director field. However, the standard methodology based on a matrix representation of the SLE operator cannot be employed anymore because a reasonable spatial discretization of the director field leads to an excessively large number of stochastic variables. Thus, the slow-motional analysis of director fluctuations requires an analytical approach.

In ref 13, such an analytical procedure has been introduced for the transverse nuclear spin relaxation of deuterium nuclei. This slow-motional theory is valid on condition that the time evolution of the stochastic variables is described by a generic multidimensional Gaussian process. As a matter of fact, such a representation can be adopted for the director field in the harmonic approximation.[9] It should be mentioned that this methodology has already been applied to the analysis of transverse nuclear spin relaxation rates measured in vesicles[14,15] and in polymeric liquid crystals.[16] An extended version of the theory is reported in ref 17.

Recently, a slow motional analysis of the effects of director fluctuations on continuous-wave (CW) ESR spectra has been presented.[18] The secular and the pseudosecular contributions resulting from the hyperfine interaction in a nitroxide spin probe have been considered, and their effect on the line-shape of a CW-ESR spectra have been analyzed. The main conclusion was that, in CW-ESR spectra, the effects of director fluctuations are hardly detectable because of the difficulty in separating their contributions to the line widths from those of the probe rotational motion as well as from the inhomogeneous broadening. As in the case of NMR transverse relaxation times, this difficulty could be overcome only by using appropriate pulsed experiments.

Two-dimensional Fourier transform electron spin resonance (2D-FT-ESR) was introduced as a technique that provides considerable enhancement in resolution to ordering and dynamics as compared to conventional ESR spectroscopy.[19] The 2D electron−electron double resonance (ELDOR) experimental data presented in ref 20 for nitroxide-labeled lipids in membrane vesicles show a dependence of the homogeneous line widths of the 2D-FT-ESR autopeaks (i.e., the diagonal peaks) on the mixing time $t_m$ in the range of microseconds. Given this order of magnitude for $t_m$, such a broadening is very likely due to the process of cooperative order director fluctuations (ODF) of the lipids in the vesicles. The opportunity to observe in real time (i.e., as a function of $t_m$) these collective motions in the 2D-ELDOR experiment was emphasized in the past experimental studies.[21,22]

These experimental findings have motivated the theoretical analysis of the effects of director fluctuations on 2D-ELDOR spectra, which is presented in this work. Basically we shall apply the same methodology as in ref 13 by neglecting the pseudosecular contributions in the spin Hamiltonian for hyperfine interactions. This approximation is justified by the results of ref 18, where it has been shown that, in ordinary conditions for director fluctuations, pseudosecular contributions to line widths are much smaller than those deriving from the purely secular terms. On the other hand, in 2D-ELDOR, these terms would contribute primarily to cross-peak development. Thus this approximation, which simplifies to a large extent the theoretical analysis, has the drawback that it cannot account for the cross-peaks. Therefore, the analysis will be confined to the autopeaks of the 2D-ELDOR spectrum and to their dependence on the mixing time. Furthermore, the theoretical results will be applied to the analysis of experimental results reported in ref 20, with the purpose not only of demonstrating that the theory is capable of reproducing the experimental trends but also to show how the proper analysis of 2D-ELDOR spectra allows the characterization of the elastic properties of the vesicles.

The paper is organized as follows. In the next section, the stochastic Liouville equation for the nitroxide probe is introduced. On this basis, in the third section, we derive a formal description of the 2D-ELDOR autopeaks in terms of the time evolution operator for the stochastic variables. In the fourth section, by assuming a multidimensional Gaussian process for the director field, explicit relations are derived for the 2D-ELDOR signal in terms of the correlation function of the transverse components of the director and its time integrals. In the following sections, these theoretical results are specified for two different models of order director fluctuations: an idealized model consisting of a simple exponential correlation function (Section 5) and the more realistic but complex model describing the director fluctuations in vesicles (and in membranes) driven by shape fluctuations (Section 6). In this latter section, the experimental results reported in ref 20 are also analyzed. The main conclusions of the study are given in the final section.

## 2. The Stochastic Liouville Equation

Let us consider a typical nitroxide spin probe dissolved in a partly ordered fluid sample (like liquid crystals or the membrane in a vesicle) with the following spin Hamiltonian that includes the Zeeman interaction, described by the **g** tensor, between the unpaired electron with spin **S** and the static magnetic field $\mathbf{B_0}$ and the hyperfine interactions, described by the **A** tensor, between the electron and the nitrogen nucleus with spin **I**[7]

$$H = \beta_e \mathbf{B_0}\cdot\mathbf{gS} + \hbar\mathbf{I}\cdot\mathbf{AS} \tag{1}$$

By introducing the laboratory frame LF = (**X**, **Y**, **Z**) with the **Z** axis along the static magnetic field, the spin Hamiltonian in the secular approximation can be written as

$$H = \beta_e B_0 g_{ZZ} + \hbar(\mathbf{a}\cdot\mathbf{I})S_Z \tag{2}$$

where we have introduced the vector **a** with components $a_J = A_{J,Z}$ for $J = X,Y,Z$.

The director field is described through its orientation $\mathbf{n}(\mathbf{r}_j)$ at an ensemble of discrete locations $\mathbf{r}_j$ centered at the smallest domains compatible with the collective nature of such a field. Only two components of the local director are independent because $|\mathbf{n}| = 1$. Accordingly we can select the following ensemble of independent stochastic variables:

$$\mathbf{Q} = (...n_x(\mathbf{r}_j), n_y(\mathbf{r}_j), ...) \tag{3}$$

By introducing the average director frame, ADF = (**x**, **y**, **z**), with the **z** axis along the average orientation of the director ($\mathbf{z} \equiv \bar{\mathbf{n}}$, implying $\bar{n}_x = \bar{n}_y = 0$), the director **n** acting on the spin probe is conveniently represented as (see Figure 1)

$$\mathbf{n} = n_x\mathbf{x} + n_y\mathbf{y} + \sqrt{1 - n_x^2 - n_y^2}\,\mathbf{z} \tag{4}$$

The magnetic interactions are modulated mainly by two types of processes: the fast rotational motion of the molecule with respect to the local director and the comparatively slower collective modes of director fluctuations. We assume the molecular tumbling is fast enough to be treated according to the motional narrowing theory,[1,2] which leads to a set of

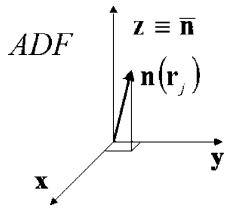


**Figure 1.** Representation of the local director in the average director frame ADF = (**x**,**y**,**z**).

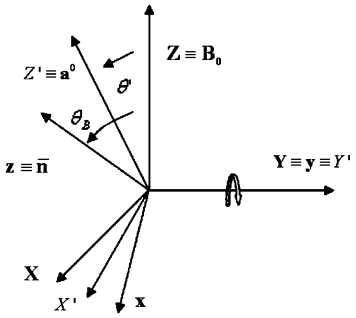


**Figure 2.** Relative orientations of the laboratory frame LF = (**X**,**Y**,**Z**), the average director frame ADF = (**x**,**y**,**z**), and the nuclear spin quantization frame NQF = (X′,Y′,Z′), together with two Euler angles ($\theta_B$,$\theta'$) used in the transformation between these frames.

relaxation times. On the other hand, the full treatment according to slow motion theory is required for the order director fluctuations. The system will be analyzed at time scales longer than the rotational correlation time so that the spin Hamiltonian averaged over the molecular orientations for a given director orientation can be used in the stochastic Liouville equation. The same notation of ref 18 will be used throughout the paper. Such an effective spin Hamiltonian is recovered from eq 1 by inserting the following orientationally averaged tensors

$$\begin{aligned} \mathbf{g} &= g_\perp \mathbf{1} + (g_{||} - g_\perp)\mathbf{n} \otimes \mathbf{n} \\ \mathbf{A} &= A_\perp \mathbf{1} + (A_{||} - A_\perp)\mathbf{n} \otimes \mathbf{n} \end{aligned} \tag{5}$$

where $g_{||}$ and $A_{||}$ ($g_\perp$ and $A_\perp$) denote their partially averaged components parallel (perpendicular) to the local director. The knowledge of the molecular tensors and of the order parameters characterizing the orientational distribution of the spin probe with respect to the local director allows one to evaluate the parallel and perpendicular components of these averaged tensors.

We choose the ADF frame with the **y** axis collinear with the **Y** axis of the LF (see Figure 2), therefore the transformation from the LF to the ADF can be specified by the Euler angles $\Omega = (0, \theta_B, 0)$, where $\theta_B$ is the angle between the static magnetic field $\mathbf{B_0}$ and the average director $\bar{\mathbf{n}}$ at the probe location. The g-tensor component required in eq 2 can be written as (**Z** is the unit vector along the static magnetic field)

$$g_{ZZ} = g_\perp + (g_{||} - g_\perp)(\mathbf{n}\cdot\mathbf{Z})^2 = g_{ZZ}^{\,0} + \delta g_{ZZ} \tag{6}$$

where $g_{ZZ}^0$ is the component in the absence of director fluctuations ($\mathbf{n} \equiv \bar{\mathbf{n}}$),

$$g_{ZZ}^{\,0} = g_\perp + (g_{||} - g_\perp)\cos^2(\theta_B) \tag{7}$$

while $\delta g_{ZZ}$ is its fluctuating part in the linear approximation with respect to the stochastic variables[13,17]

$$\delta g_{ZZ} = (g_{||} - g_\perp)\sin(2\theta_B) n_x \tag{8}$$

Clearly the average $\overline{\delta g_{ZZ}}$ vanishes because $\bar{n}_x = 0$. It should be stressed that the linear approximation holds in the case of small fluctuation amplitudes, allowing one to neglect in eq 6 higher-order terms (with respect to powers of $n_x$ and $n_y$). Notice that eq 8 leads to a vanishing $\delta g_{ZZ}$ if $\theta_B = 0°$, 90°, that is, for the so-called canonical geometries with the average director parallel or perpendicular to the magnetic field. In those situations, second-order terms have to be necessarily accounted for in the expansion of $\delta g_{ZZ}$.[17] However, in the case of vesicles where all orientations $\theta_B$ contribute, the minor correction to eq 8 due to the appearance of second-order terms can be safely ignored.

Let us now examine the hyperfine coupling term in eq 2, where the vector **a** depends on the local director **n** as

$$\mathbf{a} = A_\perp \mathbf{Z} + (A_{||} - A_\perp)(\mathbf{n}\cdot\mathbf{Z})\mathbf{n} \tag{9}$$

In the absence of director fluctuations (i.e., for $\mathbf{n} = \bar{\mathbf{n}}$), such a vector is given by (**z** is the unit vector along $\bar{\mathbf{n}}$)

$$\mathbf{a}^0 = A_\perp \mathbf{Z} + (A_{||} - A_\perp)\cos(\theta_B)\mathbf{z} \tag{10}$$

which corresponds to a vector in the (**X**, **Z**) plane of the laboratory frame (LF) with modulus

$$a^0 = |\mathbf{a}^0| = \sqrt{A_\perp^{\,2} + (A_{||}^{\,2} - A_\perp^{\,2})\cos^2(\theta_B)} \tag{11}$$

The direction of $\mathbf{a}^0$ represents the most convenient choice for the quantization axis of the nuclear spin because, in the absence of fluctuations, it leads to a diagonal representation of the spin Hamiltonian eq 2, with $a^0$ determining the hyperfine splitting. (This argument as well as eq 2 ignores the $^{14}$N nuclear Zeeman interaction, which is generally much smaller than hyperfine interactions for nitroxides, cf. refs 5−8) Thus, to specify the components of the nuclear spin operator, we introduce a further reference system, the nuclear spin quantization frame NQF = (***X***′, ***Y***′, ***Z***′), with the ***Z***′ axis oriented along $\mathbf{a}^0$ and with the ***Y***′ axis collinear with the ***Y*** axis of LF. Only the angle $\theta'$ between $\mathbf{a}^0$ and $\mathbf{B_0}$ is required to specify the relative orientation of the two reference systems (see Figure 2).

Finally, we isolate from the vector **a** of eq 9 its fluctuating part $\delta\mathbf{a} \equiv \mathbf{a} - \mathbf{a}^0$ and by invoking the linear approximation with respect the stochastic variables, we obtain

$$\delta\mathbf{a} = (A_{||} - A_\perp)[\cos(\theta_B)(n_x\mathbf{x} + n_y\mathbf{y}) - \sin(\theta_B)n_x\mathbf{z}] \tag{12}$$

By specifying the nuclear spin operator components in the NQF frame, the hyperfine interaction term can be written as

$$\mathbf{a}\cdot\mathbf{I} = a^0 I_{Z'} + (\delta a_{X'} I_{X'} + \delta a_{Y'} I_{Y'} + \delta a_{Z'} I_{Z'}) \tag{13}$$

where the fluctuating contributions to the hyperfine splitting are given by

$$\begin{aligned} \delta a_{X'} &= (A_{||} - A_\perp) n_x \cos(2\theta_B - \theta') \\ \delta a_{Y'} &= (A_{||} - A_\perp) n_y \cos(\theta_B) \\ \delta a_{Z'} &= -(A_{||} - A_\perp) n_x \sin(2\theta_B - \theta') \end{aligned} \tag{14}$$

As a further approximation, we neglect the pseudosecular contributions of hyperfine interactions and obtain the following spin Hamiltonian

$$H = \beta_e B_0 (g_{ZZ}^{\,0} + \delta g_{ZZ}) S_Z + \hbar(a^0 + \delta a_{Z'}) I_{Z'} S_Z \tag{15}$$

which is diagonal in the product $|m,M\rangle = |m\rangle|M\rangle$ between

the eigenstates $|m>$ (with $m = \pm 1/2$) and $|M>$ (with $M = 0, \pm 1$ for the $^{14}$N nitrogen of nitroxides) of electron $S_Z$ and nuclear $I_{Z'}$ spin operators, respectively. As we have already noted, such a simplification of the problem can be justified on the basis of theoretical results for the CW-ESR line widths reported in ref 18, where it has been shown that pseudosecular contributions are normally much smaller that the purely secular contributions for the case of director fluctuations. However, such an approximation means that we will not be able to describe the magnetization transfer process generating 2D-ELDOR cross-peaks, which is controlled by the pseudosecular terms of the hyperfine interaction.

The above analysis provides the effective spin Hamiltonian, eq 15, depending on the local transverse components of the director through the functions $\delta g_{ZZ}$ in eq 8 and $\delta a_{Z'}$ in eq 14. On the other hand, the dynamics of the stochastic variables are governed by the viscoelastic properties of the ordered medium. In the Markovian approximation, the time evolution of the stochastic variables is specified according to the Fokker−Planck equation for the probability density function[11,23]

$$\frac{\partial p(\mathbf{Q},t)}{\partial t} = -\Gamma_{\mathbf{Q}} p(\mathbf{Q},t) \tag{16}$$

Here $\Gamma_{\mathbf{Q}}$ denotes the time evolution operator to be modeled according to the specific viscoelastic behavior of the ordered medium, either a liquid crystal[13] or a membrane.[14] The stationary solution of eq 16 is the equilibrium distribution which will be denoted by $p_{eq}(\mathbf{Q})$.

The full description of the dynamical coupling between the spin degrees of freedom and the director fluctuations requires the solution of the stochastic Liouville equation

$$\frac{\partial \rho(\mathbf{Q},t)}{\partial t} = -\left[\frac{i}{\hbar} H(\mathbf{Q})^{\times} + \Gamma_{\mathbf{Q}} + R_{\mathrm{mol}}\right]\rho(\mathbf{Q},t) \tag{17}$$

for the $\mathbf{Q}$-dependent density matrix $\rho(\mathbf{Q},t)$ with respect to both the electron and the nuclear spin states, with $H(\mathbf{Q})^{\times}$ denoting the superoperator for commutation with the $\mathbf{Q}$-dependent Hamiltonian $H(\mathbf{Q})$. In eq 17, we have included also the molecular tumbling contribution $R_{\mathrm{mol}}$.

Because of the approximation of neglecting pseudosecular terms in the Hamiltonian, the spin degrees of freedom may be factored in the stochastic Liouville equation. Separate solutions can be written for each element of the density matrix

$$\rho^{M}_{mm'}(\mathbf{Q},t) \equiv \langle m,M|\rho(\mathbf{Q},t)|m',M\rangle = \exp\{-[i(\omega_M + \delta\omega_M)(m-m') + \Gamma_{\mathbf{Q}} + 1/T^{M}_{\gamma,\mathrm{mol}}](t-t_0)\}\rho^{M}_{mm'}(\mathbf{Q},t_0) \tag{18}$$

with $\gamma = 1$ or 2, where the longitudinal $T^{M}_{1,\mathrm{mol}}$ (the transverse $T^{M}_{2,\mathrm{mol}}$) relaxation times due to fast tumbling molecular motion have to be inserted if $m = m'$ (if $m \neq m'$). Parameters $\omega_M$ and $\delta\omega_M$ identify the resonance frequency and its fluctuating part, respectively, for the hyperfine component $M$ of the spectrum

$$\omega_M = \omega_0 + Ma^0$$
$$\delta\omega_M(\mathbf{Q}) = \beta_e B_0 \delta g_{ZZ}(\mathbf{Q})/\hbar + M\delta a_{Z'}(\mathbf{Q}) \tag{19}$$

where $\omega_0 = \beta_e B_0 g_{ZZ}{}^0/\hbar$ is the (average) Zeeman frequency of the electron spin. It should be stressed that eq 18 is only a formal solution of the stochastic Liouville equation, as long as the effects of the stochastic operator $\Gamma_{\mathbf{Q}}$ on functions of the variables $\mathbf{Q}$ is not yet evaluated. We mention also that, in this notation, $(m - m')$ represents the *coherence order* of the electron spin (that is $p^S$ in ref 19), and its allowed values are $\pm 1$, corresponding to rotating $X-Y$ components of spin magnetization, and 0 for the Z component of magnetization.

In eq 18, we have considered the diagonal elements with respect to the nuclear spin state because only these components contribute to the magnetization. Indeed, by neglecting the pseudosecular terms in the Hamiltonian, the overall magnetization $\boldsymbol{M}(t)$ can be decomposed into independent contributions

$$\boldsymbol{M}(t) = \sum_M \boldsymbol{M}^M(t) \tag{20}$$

where $\boldsymbol{M}^M(t)$ is due to the $M$th hyperfine component and can be specified as

$$\boldsymbol{M}_u{}^M(t) = -\frac{N}{V}\gamma\hbar \int \mathrm{d}\mathbf{Q}\ \mathrm{Tr}\{S_u \rho^M(\mathbf{Q},t)\} \tag{21}$$

Here $N/V$ is the spin density, the index $u$ labels the Cartesian components of the magnetization and of the spin operator, and the trace Tr{...} is calculated with respect to electron spin states only.

Similarly, the contribution of each hyperfine component can be considered independently also in the analysis of pulsed experiments, as long as the microwave pulse acts on the electron spin degrees of freedom without modifying the nuclear spin state. Therefore, in the following treatment of 2D-ELDOR experiments, we shall confine the analysis to a given hyperfine contribution with a parametric dependence on the nuclear spin quantum number $M$. Of course, the overall signal has to be evaluated as the superposition of the three hyperfine components.

Our calculation requires also the density matrix for the equilibrium state $\rho_{eq}(\mathbf{Q})$. The high-temperature approximation will be employed so that $\rho_{eq}(\mathbf{Q})$ can be specified as the product between the equilibrium distribution $p_{eq}(\mathbf{Q})$ for the stochastic variables and the equilibrium density matrix for the spin states

$$\rho_{eq}(\mathbf{Q}) \cong p_{eq}(\mathbf{Q})\frac{\exp(-\bar{H}/k_B T)}{\mathrm{Tr}\{\exp(-\bar{H}/k_B T)\}} \cong \frac{p_{eq}(\mathbf{Q})}{6}\left(1 - \frac{\hbar\omega_0}{k_B T}S_Z\right) \tag{22}$$

where the latter approximation in eq 22 holds at room temperatures for ordinary magnetic fields.

### 3. The 2D-ELDOR Spectrum

Starting from the equilibrium state, we now consider the ELDOR pulse sequence

$$\left(\frac{\pi}{2}\right)_{\phi_1} \cdots t_1 \cdots \left(\frac{\pi}{2}\right)_{\phi_2} \cdots t_m \cdots \left(\frac{\pi}{2}\right)_{\phi_3} \cdots t_2 \cdots$$

where the angle (phase) $\phi_j$ determines the axis of application of the $j$th $\pi/2$ pulse, through the conventional association $\phi_X = 0$, $\phi_Y = \pi/2$, $\phi_{-X} = \pi$, $\phi_{-Y} = 3\pi/2$. We can recognize four different time periods in a 2D-ELDOR experiment:[24] the preparation period with the first $\pi/2$ pulse to generate the initial transverse magnetization, after which the "spin packets" evolve with their characteristic frequency during the evolution period of length $t_1$. The second pulse starts the mixing period, and during this time, the longitudinal magnetization components of each hyperfine line may be exchanged in the presence of pseudosecular hyperfine interactions. Finally, the last $\pi/2$ pulse rotates the magnetization again into the $XY$ plane for detection, and the free induction decay (FID) signal is observed as a function of the detection time $t_2$.

For each hyperfine component, the detected signal depends on the lengths of the three time intervals, and it can be specified as

$$S^M_{\mathrm{ELDOR}}(t_1, t_\mathrm{m}, t_2) \propto \int \mathrm{d}\mathbf{Q}\ \mathrm{Tr}\{S_+\rho^M(t_2, t_\mathrm{m}, t_1, \mathbf{Q})\} \quad (23)$$

where $\rho^M(t_2, t_\mathrm{m}, t_1, \mathbf{Q})$ is the density matrix at the detection time. The two-dimensional spectrum is obtained by measuring the FID signal as a function of $t_2$ for a set of different values of $t_1$, and then by Fourier transforming it with respect to both of these time variables

$$\tilde{S}^M_{\mathrm{ELDOR}}(\omega_1, t_\mathrm{m}, \omega_2) = \int_0^{+\infty} \mathrm{d}t_1 \int_0^{+\infty} \mathrm{d}t_2\, e^{-i\omega_1 t_1}\, e^{-i\omega_2 t_2}\, S^M_{\mathrm{ELDOR}}(t_1, t_\mathrm{m}, t_2) \quad (24)$$

To calculate the signal, the density matrix $\rho^M(t_2, t_\mathrm{m}, t_1, \mathbf{Q})$ has to be evaluated from its initial equilibrium state $\rho_{\mathrm{eq}}(\mathbf{Q})$ through the various periods of spin dynamics of the 2D-ELDOR sequence.[19] In the following, we shall treat separately the evolution in the presence of a microwave pulse and during the free evolution period.

**Pulses.** In the presence of a microwave pulse, the evolution of the density matrix should in principle include both the effects of the pulse and of the relaxation. If the interaction with the pulse is much more intense than the fluctuating Hamiltonian term, then all the electron spins are uniformly affected by the pulse regardless of their resonance frequencies according to the Fourier theorem, which ensures that a pulse of duration $\delta$ covers a range of frequency $1/\delta$ centered at its frequency.

As long as the duration of such an intense pulse is short, the relaxation during the pulse can be ignored.[25] Let us now consider the evolution of the density matrix in a frame rotating at the same frequency as the alternating microwave field $\omega_{\mathrm{mw}}$.[26] Under these conditions, the pulse changes the density matrix according to a unitary transformation,[19] which is equivalent to an opposite rotation of the reference system. Indeed, the effect of the pulse on the density matrix can be expressed in terms of the pulse propagator superoperator as follows

$$\rho^M(t_P{}^+) = P^\dagger(\Omega)\rho^M(t_P{}^-)P(\Omega) = \mathbf{P}(\Omega)\rho^M(t_P{}^-) \quad (25)$$

where $P(\Omega)$ is the rotation operator in the Hilbert space, while $\rho^M(t_P{}^-)$ and $\rho^M(t_P{}^+)$ are the density matrixes prior to and after the pulse, respectively. The explicit form of $\mathbf{P}(\Omega)$ depends on the axis of application of the pulse. For a $(\pi/2)_\phi$ pulse, it can be specified by the following transformation of the density matrix with respect to electron spin states.

$$\mathbf{P}_\phi \begin{pmatrix} \rho^M_{\alpha\alpha} \\ \rho^M_{\beta\beta} \\ \rho^M_{\alpha\beta} \\ \rho^M_{\beta\alpha} \end{pmatrix} = \begin{pmatrix} 1/2 & 1/2 & (i/2)e^{i\phi} & -(i/2)\,e^{-i\phi} \\ 1/2 & 1/2 & -(i/2)\,e^{i\phi} & (i/2)\,e^{-i\phi} \\ (i/2)\,e^{-i\phi} & -(i/2)e^{-i\phi} & 1/2 & (1/2)\,e^{-i2\phi} \\ -(i/2)\,e^{i\phi} & (i/2)\,e^{i\phi} & (1/2)\,e^{i2\phi} & 1/2 \end{pmatrix} \begin{pmatrix} \rho^M_{\alpha\alpha} \\ \rho^M_{\beta\beta} \\ \rho^M_{\alpha\beta} \\ \rho^M_{\beta\alpha} \end{pmatrix} \quad (26)$$

where $\alpha$ and $\beta$ are the conventional notations for $m = {}^1/_2$ and $m = -{}^1/_2$ electron spin states.

**Free Evolution.** In the absence of a microwave pulse, the evolution of the density matrix in the rotating frame at the frequency $\omega_{\mathrm{mw}}$ of the microwave field is fully described by the stochastic Liouville operator $L^M(\mathbf{Q})$

$$\rho^M(\mathbf{Q}, t) = e^{-L^M(\mathbf{Q})t}\rho(\mathbf{Q}, t_0) \quad (27)$$

given as

$$L^M(\mathbf{Q}) = i(\omega_M - \omega_{\mathrm{mw}})S_Z{}^\times + i\delta\omega_M(\mathbf{Q})S_Z{}^\times + \Gamma_\mathbf{Q} + R^M_{\mathrm{mol}} \quad (28)$$

Because superoperators $L^M$ are diagonal with respect to electron spin states, the following equation can be used for the elements of the density matrix

$$\rho^M_{m,m'}(\mathbf{Q}, t) = U^M_{m,m'}(t)\rho^M_{m,m'}(\mathbf{Q}, t) \quad (29)$$

where $U^M_{m,m'}(t)$ are evolution operators acting on the stochastic variables only

$$U^M_{m,m'}(t) = \exp\{-[i(\omega_M - \omega_{\mathrm{mw}} + \delta\omega_M)(m - m') + \Gamma_\mathbf{Q} + 1/T^M_{\gamma,\mathrm{mol}}]t\} \quad (30)$$

Given the metric properties of the Liouville space generated by a complete basis set for both the spin states and the functional dependence on the stochastic variables,[18] the time domain signal eq 23 can be written as the following scalar product in this space

$$S^M_{\mathrm{ELDOR}}(t_1, t_\mathrm{m}, t_2) = (S_+{}^\dagger|\rho^M(t_2, t_\mathrm{m}, t_1, \mathbf{Q})) \propto (S_+{}^\dagger|\, e^{-L^M(\mathbf{Q})t_2}\mathbf{P}(\phi_3)\, e^{-L^M(\mathbf{Q})t_m}\mathbf{P}(\phi_2)\, e^{-L^M(\mathbf{Q})t_1}\mathbf{P}(\phi_1)S_z p_{\mathrm{eq}}(\mathbf{Q})) \quad (31)$$

By inserting the explicit form of the rotation operators, eq 26, we obtain a sum of six different time-dependent operator terms $A^M_k(t_2, t_\mathrm{m}, t_1)$, weighted by numerical factors $a_k$, which depend on the phase of the pulses[27]

$$S^M_{\mathrm{ELDOR}}(t_1, t_\mathrm{m}, t_2) = \int \mathrm{d}\mathbf{Q} \sum_{k=1}^{6} a_k A^M_k(t_2, t_\mathrm{m}, t_1)p_{\mathrm{eq}}(\mathbf{Q}) \quad (32)$$

These numerical factors and the time dependent terms, specified according to the evolution operator of eq 30, are given by

$$\begin{aligned}
a_1 &= -\frac{ie^{i\phi_1}}{8} & A^M_1(t_2, t_\mathrm{m}, t_1) &= U^M_{\beta\alpha}(t_2)U^M_{\beta\alpha}(t_\mathrm{m})U^M_{\beta\alpha}(t_1) \\
a_2 &= \frac{ie^{i(2\phi_2-\phi_1)}}{8} & A^M_2(t_2, t_\mathrm{m}, t_1) &= U^M_{\beta\alpha}(t_2)U^M_{\beta\alpha}(t_\mathrm{m})U^M_{\alpha\beta}(t_1) \\
a_3 &= \frac{ie^{i(\phi_1-\phi_2+\phi_3)}}{4} & A^M_3(t_2, t_\mathrm{m}, t_1) &= U^M_{\beta\alpha}(t_2)U^M_{\alpha\alpha}(t_\mathrm{m})U^M_{\beta\alpha}(t_1) \\
a_4 &= \frac{ie^{i(\phi_2-\phi_1+\phi_3)}}{4} & A^M_4(t_2, t_\mathrm{m}, t_1) &= U^M_{\beta\alpha}(t_2)U^M_{\alpha\alpha}(t_\mathrm{m})U^M_{\alpha\beta}(t_1) \\
a_5 &= -\frac{ie^{i(\phi_1-2\phi_2+2\phi_3)}}{8} & A^M_5(t_2, t_\mathrm{m}, t_1) &= U^M_{\beta\alpha}(t_2)U^M_{\alpha\beta}(t_\mathrm{m})U^M_{\beta\alpha}(t_1) \\
a_6 &= \frac{ie^{i(2\phi_3-\phi_1)}}{8} & A^M_6(t_2, t_\mathrm{m}, t_1) &= U^M_{\beta\alpha}(t_2)U^M_{\alpha\beta}(t_\mathrm{m})U^M_{\alpha\beta}(t_1)
\end{aligned} \quad (33)$$

To eliminate the transverse interference terms, ($A^M_1$, $A^M_2$, $A^M_5$, $A^M_6$ in the present notation), a 16-step phase cycle is performed

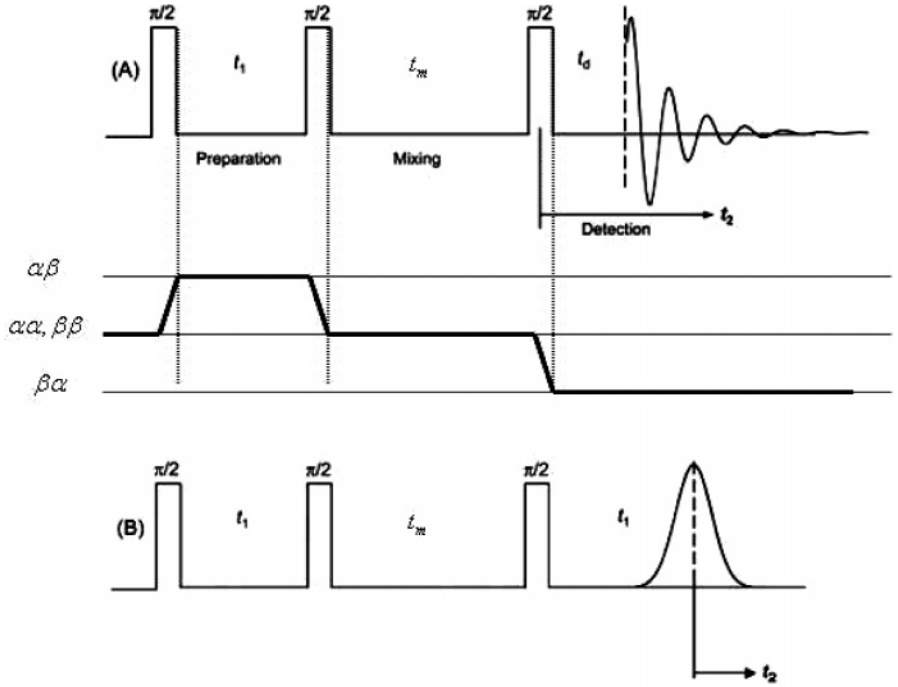


**Figure 3.** Pulse sequences and coherence transfer diagram for the (A) standard COSY mode and (B) SECSY mode of 2D-ELDOR. Notice the different definition of the time intervals in the two modes. The solid line represents the coherence pathway of the $S_{c^-}$ signal. $t_d$ denotes the spectrometer dead time and $t_m$ *i*s the mixing time.

in the experiment.[19] Then, by using the following combinations of two signals recorded by changing the first pulse phase of ($\pi$/2)

$$S^M_{c^-}(t_1, t_m, t_2) = S^M_{ELDOR}(t_1, t_m, t_2)' - iS^M_{ELDOR}(t_1, t_m, t_2)'' \quad (34)$$

only the "echo-term" $A^M_4$ (ref 19) is selected and included in the spectra. Thus, the time domain signal for a particular hyperfine line can be written as

$$S^M_{ELDOR}(t_1, t_m, t_2) = e^{-i(\omega_M-\omega_{mw})(t_1-t_2)}\, e^{-t_m/T_{1,mol}{}^M}\, e^{-(t_1+t_2)T_{2,mol}{}^M} G^M_{ELDOR}(t_1, t_m, t_2) \quad (35)$$

with the following characteristic function taking into account the effects of director fluctuations

$$G^M_{ELDOR}(t_1, t_m, t_2) = \int d\mathbf{Q}\, e^{(i\delta\omega_M-\Gamma_Q)t_2}\, e^{-\Gamma_Q t_m}\, e^{-(i\delta\omega_M+\Gamma_Q)t_1} p_{eq}(\mathbf{Q}) \quad (36)$$

The corresponding spectral density $\tilde{S}^M_{ELDOR}(\omega_1, t_m, \omega_2)$, to be evaluated according to the two-dimensional Fourier transformation eq 24, includes three peaks labeled by the index *M*, with the first exponential term at the right-hand side of eq 35 establishing their position in the ($\omega_1$, $\omega_2$) plane, while the characteristic function of eq 36 determines the director fluctuation contribution to their profile. It is easily derived that the *M*th hyperfine component is centered at the frequencies $\omega_2 = -\omega_1 = \omega_M - \omega_{mw}$, i.e., along the negative diagonal of the ($\omega_1$, $\omega_2$) plane. In general, components with different resonance frequencies, in particular, those due to inhomogeneities, are recognized along the negative diagonal of the 2D-ELDOR spectrum. Because we concentrate the analysis on the shape of a given peak, in the following, the frequency shift will be neglected by assuming that $\omega_{mw} = \omega_M$.

The structure of the characteristic function, eq 36, indicates that one is observing the "real time" motion of a spin label with the local director orientation ($n_x$, $n_y$) and a resonance frequency $\delta\omega_M$ slowly changing to a new orientation ($n_x'$,$n_y'$) with a resonant frequency $\delta\omega_M'$ during the mixing period. Because this entails a slight change in the ESR resonance frequency, a *motional cross-peak* is expected. But because the systems experience a continuum of values $\delta\omega_M'$ close in value to $\delta\omega_M$, these hypothetical cross-peaks lead to an increase in the broadening of the autopeaks depending on the length $t_m$ of the mixing period. This can be best observed by considering the SECSY (for Spin Echo Correlation Spectroscopy) mode detection of ELDOR spectra, which is depicted in Figure 3B. For the sake of comparison, Figure 3A displays the standard scheme of detection of ELDOR spectra in the COrrelation SpectroscopY (COSY) mode. Let us consider the simple case of a spin probe species characterized by inhomogeneous magnetic interactions, but in the absence of slow-motional effects, such that each spin packet has a distinct resonance frequency with a well-defined transverse relaxation time $T_2$. Then, as shown in Figure 3B, all the inhomogeneous components will be refocused to form a spin−echo at the time $t_1$ of the detection period in the SECSY mode. The signal measured afterward would result from the superposition of the FID signals of the different inhomogeneous components and, by performing the Fourier transform with respect to $t_2$, they will be separated along the corresponding frequency axis $\omega_2$. On the other hand, the homogeneous line widths will be detected along the $\omega_1$ frequency axis generated by the Fourier transform with respect to $t_1$ because, at $t_1$ in the detection period, all the inhomogeneities are refocused into the echo signal, which decays exponentially with respect to $t_1/T_2$. Therefore, the $\omega_2$ and $\omega_1$ frequency axes of the SECSY mode spectra are associated with the inhomogeneous and the homogeneous broadening of the line shape, respectively. In the COSY mode of detection the, $S_{c^-}$ signal is symmetric about the $t_1 = t_2$ axis, and this feature gives rise to the echo. In fact, a shearing transformation $t_2 \rightarrow t_1 + t_2$ recovers

the equivalent of the SECSY experiment. In other words, by considering the COSY mode of detection, the homogeneous $T_2$ may be recovered by considering the signal decay along the $t_1 = t_2$ line in the time display. We stress, however, that a clean separation between the homogeneous and the inhomogeneous broadening is missed when dealing with the effects of director fluctuations on the line shape. Indeed, because of the wide range of time scale involved in this dynamical process, there are always some fluctuating anisotropies of the spin Hamiltonian that are neither completely averaged nor completely refocused by the echo in the time scale of the experiment. As will emerge from the following analysis of collective fluctuations, we do not recover a pure exponential decay of the echo, and therefore the truly homogeneous line width associated with a Lorentzian line shape is no longer observed.

In the analysis of experimental data for vesicle systems in ref 20, the authors have evaluated the transverse relaxation times $T_2^M$ by fitting the time-dependent ELDOR signal in the SECSY format by first Fourier transforming along $t_2$ and then fitting the data along $t_1$ using linear prediction that led to the exponential function $e^{-2t/T_2{}^M}$, thereby recovering relaxation times $T_2^M(t_m)$ dependent on the mixing time $t_m$. We need to introduce also in our theoretical analysis a suitable definition of relaxation times on the basis of the time dependence of the ELDOR signal. On the basis of the analogy with the exponential model, we identify the transverse relaxation time as twice the time along the positive diagonal, (i.e. $t_1 = t_2$) in the COSY mode, which is required to reduce by a factor $1/e$ the ELDOR signal; that is the solution of the following equation

$$S^M_{\mathrm{ELDOR}}\left(\frac{T_2^M}{2}, t_m, \frac{T_2^M}{2}\right) = \frac{1}{e} \tag{37}$$

This approach and that used in ref 20 have been shown to be equivalent.[19] It should be stressed that, in the absence of director fluctuation effects, that is for $G^M_{\mathrm{ELDOR}} = 1$, the equivalence with the molecular relaxation times $T_2^M = T^M_{2,\mathrm{mol}}$ is recovered from eq 35. We mention also that the longitudinal relaxation times $T^M_{1,\mathrm{mol}}$ have no effect on the calculation of the transverse relaxation times as long as these parameters control only the dependence of the signal intensity on the mixing time $t_m$. In the frequency domain, this corresponds to the control of the peak intensities by the longitudinal relaxation times but without modifying their shape.

#### 4. Formal Solution for a Gaussian Process

To derive an explicit form of the characteristic function $G^M_{\mathrm{ELDOR}}(t_1, t_m, t_2)$, eq 36, the time evolution for the stochastic variables has to be evaluated. This can be done in a rather general way by supposing that director fluctuations constitute a multidimensional Gaussian process.

Let us assume that there exists a suitable representation of the director field in terms of normal modes associated with a transformation of the set of stochastic variables $\mathbf{Q} \rightarrow \tilde{\mathbf{Q}}$. The determination of variables $\tilde{\mathbf{Q}}$ requires the search for a representation in which the elastic free energy of the system can be written (exactly or approximately) as a sum of uncoupled evolving terms.[10,11] By applying the harmonic approximation for the elastic free energy, each contribution to the sum is actually a quadratic contribution. Therefore, the equilibrium distribution of the transformed field is written as a product of Gaussian distributions

$$p_{\mathrm{eq}}(\tilde{\mathbf{Q}}) \propto \prod_i \exp\{-\tilde{\mathbf{Q}}_i{}^2/2\sigma_i{}^2\} \tag{38}$$

As long as each normal mode evolves independently, a simple exponential decay can be assumed for its time correlation function

$$\overline{\tilde{Q}_i(0)\tilde{Q}_i(t)} = \sigma_i{}^2\, e^{-t/\tau_i} \tag{39}$$

where $\sigma_i{}^2$ and $\tau_i$ are the mean square amplitude and the relaxation time of the $i$th normal mode. If the transformation $\mathbf{Q} \rightarrow \tilde{\mathbf{Q}}$ is linear, then the fluctuations of the stochastic variable $\mathbf{Q}$ satisfy the requirement of a Gaussian multidimensional stochastic process.

According to the previous hypothesis, for the generic representation $\mathbf{Q}$ of the stochastic variables, we assume the following relations for the normalized equilibrium distribution

$$p_{\mathrm{eq}}(\mathbf{Q}) = \det(\mathbf{A}/2\pi)^{1/2} \exp(-\mathbf{Q}^\dagger \mathbf{A} \mathbf{Q}/2) \tag{40}$$

and the Fokker−Planck−Smoluchowski model[23] for the evolution operator

$$\Gamma_{\mathbf{Q}} = -\sum_{i,j} \frac{\partial}{\partial \mathbf{Q}_i} D_{ij} p_{\mathrm{eq}}(\mathbf{Q}) \frac{\partial}{\partial \mathbf{Q}_j} p_{\mathrm{eq}}{}^{-1}(\mathbf{Q}) = \left(\frac{\partial}{\partial \mathbf{Q}}\right)^\dagger \mathbf{D} p_{\mathrm{eq}}(\mathbf{Q}) \frac{\partial}{\partial \mathbf{Q}} p_{\mathrm{eq}}{}^{-1}(\mathbf{Q}) \tag{41}$$

Both the curvature matrix $\mathbf{A}$ and the diffusion matrix $\mathbf{D}$ are real, symmetric, and positive definite. Notice that the inverse of matrix $\mathbf{A}$ determines the second moments in the equilibrium state $(\mathbf{A}^{-1})_{ij} = \overline{\mathbf{Q}_i \mathbf{Q}_j}$, whereas the diffusion matrix describes the relaxation rates to equilibrium and the corresponding dynamical coupling between the stochastic variables. Because the following analysis does not require specific assumptions about the structure of the matrixes $\mathbf{A}$ and $\mathbf{D}$, the final result can be applied to different models of director fluctuations, provided that they can be represented as Gaussian processes.

Let us introduce a formal expression for the transverse component of the director field at the position $\mathbf{r}_p$ where the spin probe is located

$$F(\mathbf{Q}) = n_x(\mathbf{r}_p) = \mathbf{Q}^\dagger \mathbf{v} \tag{42}$$

where $\mathbf{v}$ is a vector with null entries except for a single value of unity corresponding to the selected element $n_x(\mathbf{r}_p)$ of the director field. This allows the explicit calculation of the correlation function for the director fluctuations at the probe location by taking into account that the evolution operator $\Gamma_{\mathbf{Q}}$ preserves the linear dependence on $\mathbf{Q}$[13]

$$\overline{n_x(0)n_x(t)} \equiv \overline{F(0)F(t)} = \int \mathrm{d}\mathbf{Q} F(\mathbf{Q})\, e^{-\Gamma_{\mathbf{Q}} t} F(\mathbf{Q}) P_{\mathrm{eq}}(\mathbf{Q}) = \mathbf{v}^\dagger\, e^{-\mathbf{D}\mathbf{A}t} \mathbf{v} \tag{43}$$

For later use, we introduce also the double time integral of this correlation function

$$g(t) \equiv \frac{1}{2} \int_0^t \mathrm{d}t' \int_0^t \mathrm{d}t \overline{n_x(t')n_x(t'')} \tag{44}$$

which corresponds to the second cumulant of the probability distribution function.

To find an explicit form for the characteristic function of eq 36, it is necessary to evaluate the effects of the evolution

operator $in\delta\omega_M(\mathbf{Q}) + \Gamma_\mathbf{Q}$, with $n = 0, \pm 1$, on a given function of the stochastic variables

$$f(\mathbf{Q},t) = e^{-(in\delta\omega_M+\Gamma_\mathbf{Q})(t-t_0)} f(\mathbf{Q},t_0) \tag{45}$$

Because of the assumed linear dependence of the Hamiltonian on the local component of the fluctuating director, a linear relation is found for the **Q**-dependence of the resonance frequency factor

$$\delta\omega_M(\mathbf{Q}) = \delta\omega_M' n_x(\mathbf{r}_p) = \delta\omega_M' \mathbf{v}^\dagger \mathbf{Q} \tag{46}$$

where the proportionality factor is given as

$$\delta\omega_M' = \frac{\beta_e B_0}{\hbar}(g_{||} - g_\perp)\sin(2\theta_B) - M(A_{||} - A_\perp)\sin(2\theta_B - \theta') \tag{47}$$

As shown in ref 13, explicit solutions of eq 45 are more easily derived by employing Fourier transformed functions with respect to the stochastic variables

$$\tilde{f}(\mathbf{p},t) \equiv \int d\mathbf{Q}\, e^{-i\mathbf{Q}^\dagger \mathbf{p}} f(\mathbf{Q},t) \tag{48}$$

which evolve in time as:

$$\frac{\partial \tilde{f}(\mathbf{p},t)}{\partial t} \equiv -\tilde{\vartheta}_{M,n} \tilde{f}(\mathbf{p},t) \tag{49}$$

with a first-order differential operator

$$\tilde{\vartheta}_{M,n} = \mathbf{p}^\dagger \mathbf{D}\mathbf{p} + (\mathbf{p}^\dagger \mathbf{D}\mathbf{A} - n\delta\omega_M' \mathbf{v}^\dagger)\frac{\partial}{\partial \mathbf{p}} \tag{50}$$

Thus, the formal solution in Fourier space can be specified as

$$\tilde{f}(\mathbf{p},t) = e^{-\tilde{\vartheta}_{M,n}(t-t_0)} \tilde{f}(\mathbf{p},t_0) \tag{51}$$

and by noting that the Fourier transform of the equilibrium distribution is given by

$$\tilde{p}_{eq}(\mathbf{p}) = \exp(-\mathbf{p}^\dagger \mathbf{A}^{-1}\mathbf{p}/2) \tag{52}$$

the characteristic function eq 36 is written as

$$G^M_{ELDOR}(t_1, t_m, t_2) = [e^{-\tilde{\vartheta}_{M,-1}t_2}\, e^{-\tilde{\vartheta}_{M,0}t_m}\, e^{-\tilde{\vartheta}_{M,1}t1}\exp(-\mathbf{p}^\dagger \mathbf{A}^{-1}\mathbf{p}/2)]_{\mathbf{p}=\mathbf{0}} \tag{53}$$

Given the first-order character of the transformed operators $\tilde{\vartheta}_{M,n}$, the explicit solution can be obtained using standard procedures for ordinary differential equations. Let us consider the following trial function

$$\tilde{f}(\mathbf{p},t) = \exp\{-a(t) - \mathbf{p}^\dagger \mathbf{b}(t) - \mathbf{p}^\dagger \mathbf{A}^{-1}\mathbf{p}/2\} \tag{54}$$

which represents a shifted Gaussian with the same widths as the transformed equilibrium distribution, eq 52, while its center and intensity are allowed to change in time because of the effects of the evolution operator. As shown in ref 13, it can be easily verified that such a trial function is a particular solution of eq 49 associated with eq 52 as the initial state. In particular, the substitution of the trial function into the time evolution eq 49 and the separation of the terms with the same power of **p**, leads to ordinary differential equations of the first order for the time-dependent parameters $a(t)$ and $\mathbf{b}(t)$, which can be integrated as

$$\mathbf{b}(t) = e^{-\mathbf{D}\mathbf{A}(t-t_0)}\mathbf{b}(t_0) - n\delta\omega_M' \int_0^{t-t_0} e^{-\mathbf{D}\mathbf{A}t'}\mathbf{A}^{-1}\mathbf{v}\, dt'$$
$$a(t) = a(t_0) - n\delta\omega_M' \int_{t_0}^{t} \mathbf{v}^\dagger \mathbf{b}(t')\, dt' \tag{55}$$

where $a(t_0)$ and $\mathbf{b}(t_0)$ are the generic initial conditions.

Such an integration scheme can be applied to the ELDOR characteristic function in the Fourier transform representation, eq 53. For the initial state described by the equilibrium distribution, eq 52, vanishing values of the integration parameters have to be considered

$$a(0) = 0, \qquad \mathbf{b}(0) = \mathbf{0} \tag{56}$$

Starting from this initial condition, we can evaluate the evolution of the function eq 51 during the first period of length $t_1$. Then, the function at time $t_1$ is taken as the initial condition for the evolution during $t_m$. Again, its final state represents the initial condition for the evolution during $t_2$. In detail, we obtain

(i) Evolution during $t_1$ controlled by $\tilde{\vartheta}_{M,-1}$

$$\mathbf{b}(t_1) = \delta\omega_M' \int_0^{t_1} e^{-\mathbf{D}\mathbf{A}t_1'}\mathbf{A}^{-1}\mathbf{v}\, dt_1'$$
$$a(t_1) = (\delta\omega_M')^2 \int_0^{t_1} dt_1' \int_0^{t_1'} dt_1'' \mathbf{v}^\dagger\, e^{-\mathbf{D}\mathbf{A}t_1''}\mathbf{A}^{-1}\mathbf{v} = (\delta\omega_M')^2 g(t_1)$$

where $g(t)$ is given by eq 44.

(ii) Evolution during $t_m$ controlled by $\tilde{\vartheta}_{M,0}$

$$\mathbf{b}(t_m, t_1) = e^{-\mathbf{D}\mathbf{A}t_m}\mathbf{b}(t_1)$$
$$a(t_m, t_1) = a(t_1)$$

(iii) Evolution during $t_2$ controlled by $\tilde{\vartheta}_{M,1}$

$$\mathbf{b}(t_2, t_m, t_1) = e^{-\mathbf{D}\mathbf{A}t_2}\mathbf{b}(t_m, t_1) - \delta\omega_M' \int_0^{t_2} e^{-\mathbf{D}\mathbf{A}t_2'}\mathbf{A}^{-1}\mathbf{v}\, dt_2'$$
$$a(t_2, t_m, t_1) = (\delta\omega_M')^2[g(t_1) + g(t_2) - g_{1,2}(t_1 + t_m + t_2)]$$

where

$$g_{1,2}(t_1, t_m, t_2) \equiv \int_0^{t_2} dt_2' \int_0^{t_1} dt_1' \mathbf{v}^\dagger\, e^{-\mathbf{D}\mathbf{A}(t_2'+t_m+t_1')}\mathbf{A}^{-1}\mathbf{v} = \int_0^{t_2} dt_2' \int_0^{t_1} dt_1' \overline{n_x(0)n_x(t_1' + t_m + t_2')} \tag{57}$$

In conclusion, according to eq 53, the $G^M_{ELDOR}(t_1, t_m, t_2)$ function can be specified as

$$G^M_{ELDOR}(t_1, t_m, t_2) = e^{-a(t_1,t_m,t_2)} = \exp\{-(\delta\omega_M')^2[g(t_1) + g(t_2) - g_{1,2}(t_1, t_m, t_2)]\} \tag{58}$$

and, therefore, the knowledge of the correlation function $\overline{n_x(0)n_x(t)}$ for the local transverse component of the director, is sufficient for predicting the effects of collective order fluctuations on these pulsed ESR experiments. A similar conclusion was drawn also for NMR pulsed experiments by analyzing the effects of director fluctuations on quadrupolar interactions.[13] We emphasize this is strictly a consequence of the assumption of Gaussian random processes.

It should be stressed that, because of the contribution of $g_{1,2}(t_1, t_m, t_2)$, the characteristic function $G^M_{ELDOR}$ and the corresponding contribution to the line widths depend on the mixing time $t_m$. Notice that the contribution of $g_{1,2}(t_1, t_m, t_2)$

decreases when $t_m$ is increased, as long as the correlation function

$$\overline{n_x(0)n_x(t)}$$

of director fluctuations is a continually decreasing function of the time. In particular, for $t_m \rightarrow \infty$, such a contribution necessarily vanishes, and the signal becomes the product of two independent FID signals,[18] one recorded during $t_1$ and the other during $t_2$.

### 5. Model Calculations

To illustrate, by a simple model, the effects of collective order fluctuations on the 2D-ELDOR spectra, let us consider the hypothetical case of director fluctuations with local components decaying as a simple exponential

$$\overline{n_x(0)n_x(t)} = \overline{n_x^2}e^{-t/\tau} \tag{59}$$

Then the time integrals of the correlation function, which have been previously introduced, take the explicit form

$$g(t) = \overline{n_x^2}\tau^2(e^{-t/\tau} - 1 + t/\tau) \tag{60}$$

$$g_{12}(t_1, t_m, t_2) = \overline{n_x^2}\tau^2 e^{-t_m/\tau}(1 - e^{-t_1/\tau})(1 - e^{-t_2/\tau}) \tag{61}$$

Even in this simple case, a complex time behavior is found for the characteristic function $G^M_{\mathrm{ELDOR}}(t_1, t_m, t_2)$, which cannot be reproduced by an exponential decay. Therefore, definition eq 37 will be employed to calculate the transverse relaxation time $T_2^M$ and to evaluate its dependence on the mixing time $t_m$. The simple structure of the model suggests the use of the fluctuation amplitude of the resonance frequency

$$\Delta\omega_M = |\delta\omega_M'|\sqrt{\overline{n_x^2}} \tag{62}$$

as the scaling factor for time variables (or the inverse for a frequency). By using the corresponding scaled variables, in the following denoted by symbols with a tilde

$$\begin{aligned} \tilde{\omega}_i &= \omega_i/\Delta\omega_M \qquad i = 1, 2 \\ \tilde{t}_i &= \Delta\omega_M t_i \qquad i = 1, 2, m \\ \tilde{\tau} &= \Delta\omega_M \tau \\ \tilde{T}_2^M &= \Delta\omega_M T_2^M \end{aligned} \tag{63}$$

it is shown that only two independent parameters need to be specified in the model: the scaled decay time $\tilde{\tau}$, characterizing the collective dynamics, and the scaled relaxation time $\tilde{T}^M_{2,\mathrm{mol}}$ due to the molecular tumbling.

First, let us discuss the main features of the derived ELDOR signal in the ideal limit of a vanishing molecular tumbling contribution to the relaxation rate $(\tilde{T}^M_{2,\mathrm{mol}})^{-1} = 0$, so that the relaxation time is completely determined by the collective dynamics and $S^M_{\mathrm{ELDOR}}(\tilde{t}_1, \tilde{t}_m, \tilde{t}_2) = G^M_{\mathrm{ELDOR}}(\tilde{t}_1, \tilde{t}_m, \tilde{t}_2)$ according to eq 35. In such a situation, the magnetization evolution is entirely due to the director fluctuations (DF) and, therefore, the corresponding transverse relaxation time will be denoted as $T^M_{2,\mathrm{DF}}$. Figure 4 shows the characteristic function for two different values of the mixing time. Notice that a faster decay of the time signal is obtained for longer $\tilde{t}_m$; however, there is no dependence on the mixing time along the two time axes,

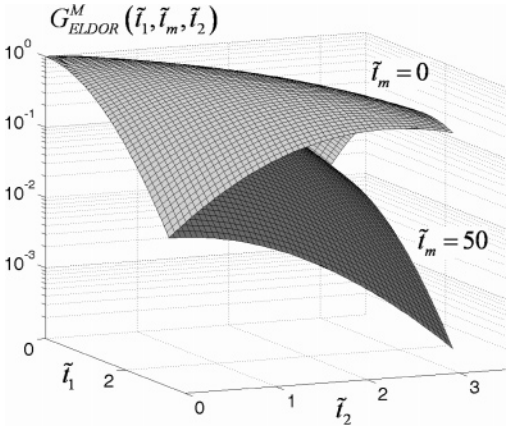


**Figure 4.** Time dependence of the characteristic function $G^M_{\mathrm{ELDOR}}(\tilde{t}_1,\tilde{t}_m,\tilde{t}_2)$ of the ELDOR experiment, characterizing the director fluctuation contribution to the relaxation process for the model of a single-exponential correlation function. The time profiles refer to a scaled decay time of $\tilde{\tau} = 10$ and two different values of the scaled mixing time, i.e., $\tilde{t}_m = 0$ (upper plot) and $\tilde{t}_m = 50$ (lower plot).

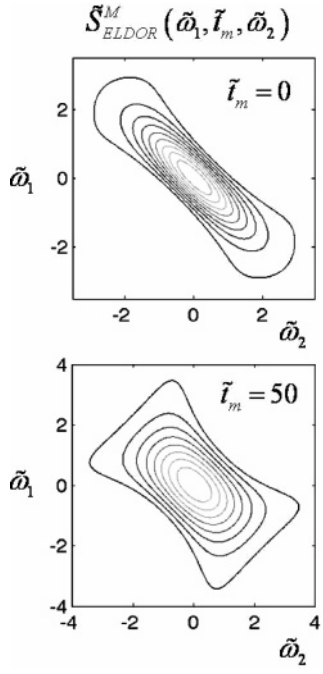


**Figure 5.** Contour plots of the absorption profile $\mathrm{Re}[\tilde{S}^M_{\mathrm{ELDOR}}(\tilde{\omega}_1,\tilde{t}_m,\tilde{\omega}_2)]$ of the ELDOR experiment characterizing director fluctuations for the model of a single-exponential correlation function. The contour plots refer to a scaled decay time of $\tilde{\tau} = 10$ and two different values of the scaled mixing time, i.e., $\tilde{t}_m = 0$ (upper plot) and $\tilde{t}_m = 50$ (lower plot).

i.e., for $\tilde{t}_1 = 0$ or $\tilde{t}_2 = 0$. Indeed, for these special cases $g_{1,2} = 0$ and the function $G^M_{\mathrm{ELDOR}}$ is equivalent to the secular part of the FID signal derived in ref 16. Furthermore, the relaxation function decays more slowly along the $\tilde{t}_1 = \tilde{t}_2$ axis, in agreement with the echo property of the signal as discussed in the previous section.

By examining the spectral density $\tilde{S}^M_{\mathrm{ELDOR}}(\tilde{\omega}_1, \tilde{t}_m, \tilde{\omega}_2)$, defined according to eq 24, one can detect the effects of director fluctuation on the line shapes. Contour plots of the absorption profile, obtained as the real part of $\tilde{S}^M_{\mathrm{ELDOR}}(\tilde{\omega}_1, \tilde{t}_m, \tilde{\omega}_2)$, are depicted in Figure 5. Even in the COSY spectrum, where the spectral direction associated with the homogeneous line width is not well defined as in the SECSY spectrum, a narrowing of the line width is clearly observed when the frequency displacement is considered along the positive diagonal. Furthermore,

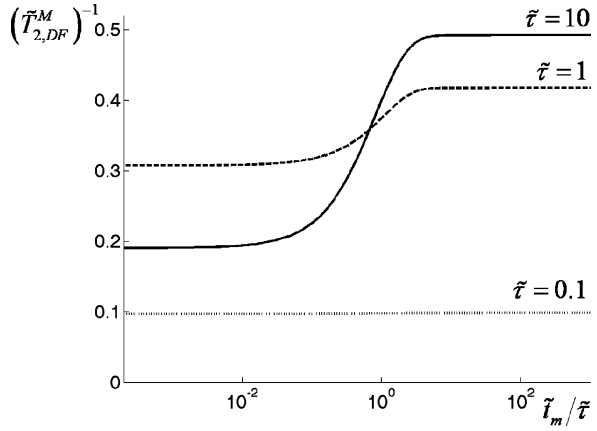


**Figure 6.** Dependence of the scaled transverse relaxation rate $(\tilde{T}^M_{2,DF})^{-1}$, arising from director fluctuations, on the scaled mixing time $t_m/\tilde{\tau}$ for three different values of the scaled decay time $\tilde{\tau}$ for the director fluctuation described by the model of a single-exponential correlation function. The relaxation curves refer to a vanishing molecular contribution, i.e., $(\tilde{T}^M_{2,mol})^{-1} = 0$.

the line width in this direction increases with the mixing time because the inhomogeneities modulated by director fluctuations are not completely refocused and, therefore, significant deviations from the Lorentzian shape are expected.

Let us now analyze the mixing time dependence of the transverse relaxation time $T^M_{2,DF}$ in the absence of the molecular tumbling contribution. In Figure 6, such a dependence is illustrated in some typical conditions. The simplest case is that of the *motional narrowing regime* where the rate $1/\tau$ of the dynamical process is much larger than the fluctuation amplitude $\Delta\omega_M$ eq 62 of the resonance frequencies

$$1/\tau \gg \Delta\omega_M \tag{64}$$

or $\tilde{\tau} \ll 1$ in scaled units. The case for $\tilde{\tau} = 0.1$ in Figure 6 is representative of such a situation when no dependence on the mixing time is detected for the transverse relaxation time. From the $\tilde{\tau} \to 0$ expansion in eqs 60−61, one derives the following analytical approximation of the characteristic function

$$G^M_{ELDOR}(\tilde{t}_1,\tilde{t}_2) \cong \exp[-\tilde{\tau}(\tilde{t}_1 + \tilde{t}_2)] \tag{65}$$

which leads to a transverse relaxation time independent of the mixing time

$$1/\tilde{T}^M_{2,DF} = \tilde{\tau} \tag{66}$$

It should be mentioned that, because of the exponential decay found in this case for $G^M_{ELDOR}$, a Lorentzian line shape representation of a truly homogeneous process is recovered in the frequency domain.

If the condition (eq 64) is not satisfied, that is for

$$1/\tau \lesssim \Delta\omega_M \tag{67}$$

(or $\tilde{\tau} \gtrsim 1$ in scaled units), the system falls in the *slow motion regime* and a mixing time dependence is detected for the transverse relaxation time. The two cases for $\tilde{\tau} = 1$ and $\tilde{\tau} = 10$, displayed in Figure 6, clearly show such a dependence and, furthermore, point out that changes of the transverse relaxation time are detected when the mixing time is in the same range as the correlation time $\tau$ of the dynamical process controlling the resonance frequency fluctuations. This appears to be a rather general result, which implies that, if $(T^M_2)^{-1}$ displays a $t_m$ dependence within some time window, then there should be a slow fluctuating component with about the same time scale. Analytical estimates of the transverse relaxation times for situations where no dependence on the mixing time is observed can be obtained for $\tilde{\tau} \gg 1$ by performing a suitable expansions of the functions eqs 60−61 with the following results

$$\tilde{t}_m \gg \tilde{\tau} \qquad (T^M_{2,DF})^{-1} = (1/2) \tag{68}$$

$$\tilde{t}_m \ll \tilde{\tau} \qquad (T^M_{2,DF})^{-1} = (12\tilde{\tau})^{-1/3} \tag{69}$$

We mention also that by performing the $\tilde{\tau} \to \infty$ limit, the *rigid limit* is recovered with a characteristic function given as

$$G^M_{ELDOR}(\tilde{t}_1,\tilde{t}_2) \cong \exp[-(\tilde{t}_2 - \tilde{t}_1)^2/2] \tag{70}$$

corresponding to a Gaussian inhomogeneous broadening which is refocused for $\tilde{t}_1 = \tilde{t}_2$ because of the echo property of the signal.

Let us finally examine the effect of the molecular contribution $T^M_{2,mol}$, treated within the fast motional regime, on the mixing time dependence of the transverse relaxation time $T^M_2$. A very simple case to analyze is that for the motional narrowing regime under the condition (eq 64), where additive contributions from the molecular tumbling and director fluctuations result for the time dependent ELDOR signal eq 35,

$$\frac{1}{T^M_2} = \frac{1}{T^M_{2,DF}} + \frac{1}{T^M_{2,mol}} \tag{71}$$

In this case, no mixing time dependence is detected on the transverse relaxation time. A more interesting situation is that of the slow motion regime, under the condition (eq 67), when such a simple additive relation is no more valid. Still, some general conclusions are easily derived from the basic structure of eq 35 for the time- dependent ELDOR signal. Given the director fluctuation contribution $T^M_{2,DF}$ previously discussed, one can recognize the two obvious limits

$$\text{(i)}\ \frac{1}{T^M_{2,DF}} \gg \frac{1}{T^M_{2,mol}} \qquad \frac{1}{T^M_2} \cong \frac{1}{T^M_{2,DF}}$$

$$\text{(ii)}\ \frac{1}{T^M_{2,DF}} \ll \frac{1}{T^M_{2,mol}} \qquad \frac{1}{T^M_2} \cong \frac{1}{T^M_{2,mol}}$$

When the two rates, $(T^M_{2,DF})^{-1}$ and $(T^M_{2,mol})^{-1}$, have a comparable magnitude, then the solution of eq 37 is required in order to evaluate the overall transverse relaxation time $T^M_2$. Figure 7 reports some typical results for the mixing time dependence of $(T^M_2)^{-1}$ calculated with $\tilde{\tau} = 10$ and increasing values of the molecular tumbling contribution. It is evident that, when the molecular tumbling prevails, that is if the condition (ii) holds, the mixing time dependence is completely lost. Such a dependence is indeed detectable if the molecular tumbling contribution $(T^M_{2,mol})^{-1}$ is comparable to or smaller than the director fluctuation component $(T^M_{2,DF})^{-1}$, provided that the slow motion condition eq 67 holds.

### 6. Application to Vesicle Samples

Biological membranes exhibit exceptional mechanical properties unequalled by any other soft condensed matter material.[28] A crucial parameter determining the shape fluctuations and functionality of closed biomembranes is the bending elastic modulus $\kappa$. Similar to order director fluctuations in nematic

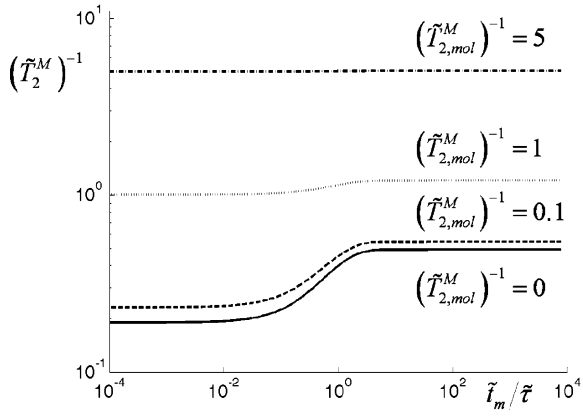


**Figure 7.** Dependence of the scaled overall transverse relaxation rate $(\tilde{T}_2^M)^{-1}$ on the ratio $\tilde{t}_m/\tilde{\tau}$ between the scaled mixing time and the scaled decay time of the model correlation function with a single exponential. The relaxation profiles, each labeled by the assumed value of the molecular tumbling contribution $(\tilde{T}_{2,mol}^M)^{-1}$ in scaled units, are calculated for a scaled relaxation time of $\tilde{\tau} = 10$.

phases, the shape fluctuations in closed lipid bilayers are characterized by a broad distribution of thermally activated modes extending over a wide frequency range down to the kHz regime.[15] It was shown that the transverse $^{31}$P nuclear spin relaxation rates, measured in Carr−Purcell multipulse sequences, are the same for unilamellar and oligolamellar vesicles.[15] Evidently, the interbilayer coupling is much weaker than previously anticipated[29,30] and has no effect on the membrane fluctuations down to the kHz range. Therefore, in the case of multilamellar vesicles in excess water, where interbilayer water significantly reduces the coupling between the layers, the shape fluctuations are expected to be comparable to those of unilamellar vesicles.[31,32] For this reason, the hydrodynamic model, developed for the analysis of unilamellar vesicles,[14] can also be used for oligolamellar vesicles explored in the experiment of ref 20.

The model calculations in this section are reported for a spin probe in a vesicle in order to describe the effect of director fluctuations on the 2D-ELDOR relaxation rates $(T_2^M)^{-1}$. First, a specific spin probe in a given membrane vesicle sample is chosen in order to evaluate the relevant hyperfine frequencies and their angular dependence. Second, we summarize the standard model for the fluctuations of quasispherical vesicles to provide an explicit relation for the required correlation function.[14] On the basis of these results, we shall analyze the relaxation of the magnetization by considering the purely secular contribution of the director fluctuations. This allows the characterization of their specific features as well as their relevant dependence on the mixing time $t_m$. Finally, we discuss the so-called MOMD effect:[19] these vesicles samples are characterized by the lipids being microscopically ordered at a given position of the vesicle, but the sample is macroscopically disordered because of the orientational distribution of the normal direction of the membrane. This leads to a superposition of spectra from membrane fragments with different orientations.

A complete characterization of these spectra also requires the relaxation rates $(T_{2,mol}^M)^{-1}$ due to the fast molecular tumbling. Although these rates can be evaluated according to a diffusion model in the presence of an orienting potential,[7,33] they will simply be parametrized in order to avoid a too cumbersome presentation and to focus attention on the contribution of the director fluctuations.

**The Magnetic Parameters of the Spin Probe.** To carry out calculations pertinent to a realistic situation, we choose the spin probe 16-PC (1-palmitoyl-2-(16-doxyl stearoyl) phosphatidylcholine) dissolved in vesicles of DPPC (1,2-dipalmitoyl-*sn*-glycero-phosphatidylcholine). The 2D-ELDOR spectra of this nitroxide radical have been analyzed in detail by Patyal at al.[20] in order to study the effects of adding gramicidin A′ (GA) to the DPPC membrane. The spectra have been recorded at X-band (9.25GHz), which corresponds to a static magnetic field of $B_0 = 3300$ *G*. Table 1 summarizes the principal values for the *g*-tensor and hyperfine tensor of the nitroxide radical, obtained for 16-PC in pure DPPC vesicles and in DPPC/GA mixed vesicles (molar ratio 5:1). The orientation of the principal axes of the magnetic tensors is depicted in Figure 8 together with the chemical structure of the spin probe.

**TABLE 1: Magnetic and Order Parameters of the Spin Probe 16-PC[a] Used to Study the Viscoelastic Properties of Pure DPPC[b] Vesicles and of Mixed DPPC/GA[c] Vesicles by 2D-ELDOR[d]**

| $T = 318$ K | 16-PC in DPPC | 16-PC in DPPC/GA (5:1) |
|---|---|---|
| $g_{xx}$ | 2.0089 | 2.0087 |
| $g_{yy}$ | 2.0058 | 2.0059 |
| $g_{zz}$ | 2.0021 | 2.0021 |
| $A_{xx} = A_{yy}$ (G) | 5.0 | 5.0 |
| $A_{zz}$ (G) | 33 | 33.7 |
| $S_0$ | 0.183 | 0.218 |
| $S_2$ | −0.049 | −0.064 |
| $S_{xx}$ | −0.123 | −0.1482 |
| $S_{yy}$ | −0.063 | −0.0698 |
| $S_{zz}$ | 0.183 | 0.2180 |
| $A_{\|\|}$ (G) | 17.81 | 18.74 |
| $A_\perp$ (G) | 12.60 | 12.48 |
| $g_{\|\|}$ | 2.0049 | 2.0047 |
| $g_\perp$ | 2.0060 | 2.0060 |

[a] 16-PC: (1-palmitoyl-2-(16-doxylstearoyl)phosphatidylcholine). [b] DPPC: (1,2-dipalmitoyl-*sn*-glycero-phosphatidylcholine). [c] GA: gramicidin A′. [d] Experimental values adopted from ref 20.

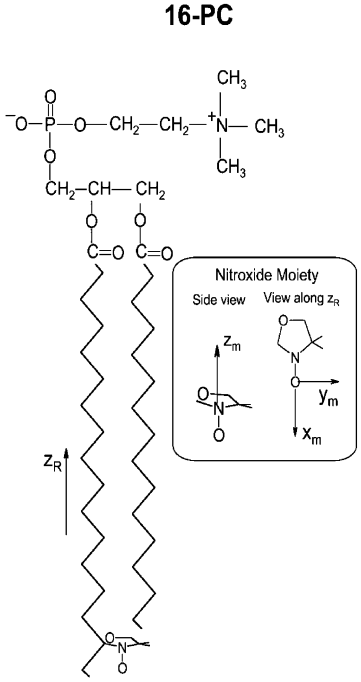


**Figure 8.** Chemical structure of the employed spin probe (1-palmitoyl-2-(16-doxylstearoyl)phosphatidylcholine). Also depicted is the orientation of the principal axes of the magnetic tensors ($\mathbf{x}_m$,$\mathbf{y}_m$,$\mathbf{z}_m$). $\mathbf{Z}_R$ = principal axis of the ordering matrix.

In ref 20, the axial order parameter $S_0 = \overline{D_{0,0}^2}$ and the biaxial order parameter $S_2 = \overline{D_{0,2}^2} + \overline{D_{0,-2}^2}$ of the spin probe in pure DPPC vesicles and in DPPC/GA mixed vesicles are

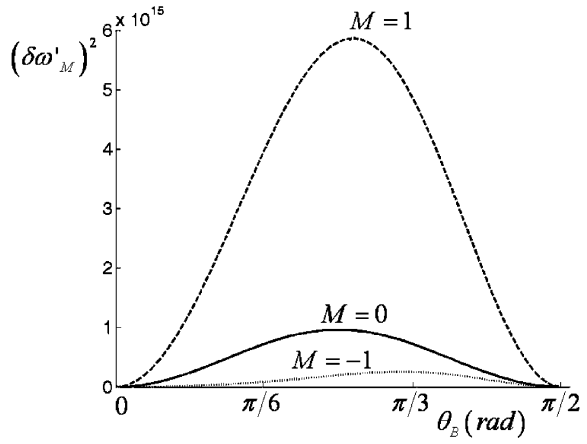


**Figure 9.** Angular dependence of the coefficients $\delta\omega'_M{}^2(\theta_B)$ characterizing the strength of the director fluctuation contribution to the relaxation for the examined spin probe.

reported. The order parameters refer to a temperature of 45 °C and are directly related to the Cartesian components $S_{ij}$ of the Saupe ordering matrix, characterizing the alignment of the molecular axes with respect to the local director. On the assumption that the magnetic tensors and the Saupe ordering matrix have the same principal axes, one can calculate the parallel and perpendicular components of the averaged *g*-tensor

$$g_{\parallel} = \sum_{j=x,y,z} g_{jj}\frac{1+2S_{jj}}{3} \qquad g_{\perp} = \sum_{j=x,y,z} g_{jj}\frac{1-2S_{jj}}{3} \quad (72)$$

and the averaged components $A_{\parallel}$ and $A_{\perp}$ of the hyperfine tensor as well. Given these averaged tensors, we can calculate the coefficients $\delta\omega_M'$ in eq 47, which determine the weights of order director fluctuations on the ELDOR observables. Figure 9 depicts the dependence of these coefficients on the angle $\theta_B$ between the average director and the magnetic field. Notice that the angle $\theta'$ in eq 47 is calculated for each $\theta_B$ according to eq 10. One sees that the coefficients $(\delta\omega_0')^2$ and $(\delta\omega_{-1}')^2$ are much smaller than $(\delta\omega_1')^2$, which reaches its maximum value at $\theta_B \approx \pi/4$. Consequently, the largest effect of the director fluctuations on the ELDOR line widths is expected for the $M = 1$ hyperfine line at a director orientation of $\theta_B \approx \pi/4$. It should be noted that only linear contributions of the orthogonal components of the fluctuating director have been employed in the analysis. Thus, the theory cannot account for canonical orientations, $\theta_B = 0$ and $\theta_B = \pi/2$, where the average director is either parallel or perpendicular to the magnetic field.

**Fluctuations of Quasispherical Vesicles.** The model of quasispherical fluctuations was developed by Milner and Safran[34] on the basis of Helfrich's theory of the elasticity of lipid bilayers[35] and the hydrodynamic approach of Schneider et al.[36] In this model, a vesicle is considered to be a quasispherical closed shell of radius $R_0$ characterized by a fixed volume $V$ and a fixed area $A$. The vesicle is assumed to be flaccid, with the dimensionless excess area $\Delta$ describing the deviation of the vesicle from a sphere of the same volume:

$$A = (4\pi + \Delta)R_0^2 \quad (73)$$

For a quantitative modeling of the fluctuations, the vesicle is described by a slightly deformed spherical surface as (see Figure 10)

$$R(\theta, \phi) = R_0(1 + u(\theta, \phi)) \quad (74)$$

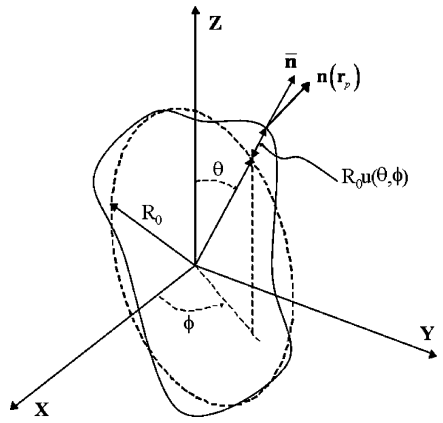


**Figure 10.** Schematic representation of the shape fluctuations of quasispherical vesicles. $\theta$ and $\phi$ denote the polar and azimuthal angles, respectively, of the considered surface point with respect to an arbitrary reference system. $R_0u(\theta,\phi)$ characterizes the radial deviation from the spherical geometry.

where $u(\theta, \phi)$ is a dimensionless parameter characterizing the radial deviation from the spherical geometry, while $\theta$ and $\phi$ denote the polar and azimuthal angles of the considered surface point with respect to an arbitrary reference system. The angular dependent function $u(\theta, \phi)$ can be expanded with respect to the spherical harmonics $Y_{l,m}(\theta, \phi)$ according to

$$u(\theta, \phi) = \sum_{l=2}^{l_{max}} \sum_{m=-l}^{l} u_{l,m} Y_{l,m}(\theta, \phi) \quad (75)$$

where, because of the finite size of the vesicle, the expansion has to be truncated at an upper limit $l_{max}$ of the index $l$, given by[34]

$$l_{max} \approx \frac{\pi R_0}{a} \quad (76)$$

$a$ being the typical distance between adjacent phospholipids. The expansion coefficients $u_{l,m}$ represent the normal modes for the thermal fluctuations of quasispherical vesicles, and they are characterized by independent correlation functions[34]

$$\overline{u_{l,m}(0)u_{l',m'}(t)} = \delta_{l,l'}\delta_{m,m'}\overline{u_{l,m}{}^2}\, e^{-t/\tau_l} \quad (77)$$

where the mean-square amplitude $\overline{u_{l,m}{}^2}$ and the relaxation time $\tau_l$ for each mode are given as

$$\overline{u_{l,m}{}^2} = \overline{u_l^2} = \frac{k_B T}{\kappa}\frac{1}{(l+2)(l-1)(l^2+l+\sigma)}$$

$$\tau_l = \frac{\eta R_0^3}{\kappa}\frac{(2l+1)(2l^2+2l-1)}{(l-1)l(l+1)(l+2)(l^2+l+\sigma)} \quad (78)$$

respectively. Here, $\eta$ is the viscosity of the surrounding fluid, $\kappa$ is the bending elastic modulus of the membrane, while $\sigma$ is the dimensionless effective lateral tension, which is related to the excess area $\Delta$ by the relation[37]

$$\Delta = \frac{k_B T}{2\kappa}\sum_{l=2}^{l_{max}}\frac{2l+1}{l^2+l+\sigma} \quad (79)$$

**TABLE 2: Values of Physical Parameters Used in Model Calculations of ELDOR Observables Determined by Vesicle Shape Fluctuations**

| | |
|---|---|
| $R_0$ vesicles radius, nm | 1000 |
| $\kappa$ bending elastic modulus, J | $13 \times 10^{-20}$ |
| $k_BT$ thermal energy, J ($T = 318$ K) | $4.4 \times 10^{-21}$ |
| $\eta$ viscosity, Pa s | $6.5 \times 10^{-4}$ |
| $\sigma$ lateral tension | 0 |
| $a$ intermolecular distance, nm | 1 |

Ref 14 reports the derivation of the time autocorrelation function of the transverse component of the local director defined as the orthogonal direction to the fluctuating membrane at a given position. We recall here only the final result for the correlation function of the transverse component of the director at a given position

$$\overline{n_x(0)n_x(t)} = \frac{1}{8\pi}\sum_{l=2}^{l_{max}} l(l+1)(2l+1)\overline{u_l^2}\, e^{-t/\tau_l} \qquad (80)$$

By performing a suitable double integration over the time variables, the functions $g(t)$ (eq 44) and $g_{1,2}(t_1, t_m, t_2)$ (eq 57) are easily derived, and from them, the characteristic function $G_{ELDOR}(t_1, t_m, t_2)$ describing the ELDOR experiment.

**ELDOR Line Shape and Transverse Relaxation Time.** To demonstrate the effect of vesicle shape fluctuations on the ELDOR observables, we first show representative calculations of the characteristic function $G^M_{ELDOR}$ based on the parameters listed in Table 2. The value for the bending elastic modulus $\kappa$ is adopted from the literature. The value for $\eta$ corresponds to the viscosity of water. For the effective lateral tension, values in the range $0 \le \sigma \le 100$ have been reported.[28] For simplicity, a value of $\sigma = 0$ is assumed.

We recall that the characteristic function $G^M_{ELDOR}(t_1, t_m, t_2)$ depends on the magnetic parameters only through the coefficient $(\delta\omega_M')^2$, whose angular dependence has been already examined in Figure 9. One can easily deduce the effects of changing the coefficient $(\delta\omega_M')^2$ for a given model of director fluctuations. Clearly, an increase of $(\delta\omega_M')^2$ leads to a faster relaxation of the magnetization described by $G^M_{ELDOR}(t_1, t_m, t_2)$, and correspondingly to a broader line shape $S^M_{ELDOR}(\omega_1, t_m, \omega_2)$ in the ELDOR spectrum. We concentrate here the analysis for a fixed coefficient $(\delta\omega'_M)^2 = 5.8 \times 10^{15}$ s$^{-2}$, which corresponds to a maximum value for the hyperfine line $M = 1$. In Figure 11, the time dependence of $G^M_{ELDOR}(t_1, t_m, t_2)$ is displayed for two different values of the mixing time. Although the model describing fluctuations of quasispherical vesicles is more complex than the simple exponential model considered in Section 5, the characteristic ELDOR function displays the same main features. Accordingly, the effects of director fluctuations can be well characterized through transverse relaxation times $T_2^M$ defined in eq 37

Calculations of the characteristic function $G^M_{ELDOR}(t_1, t_m, t_2)$ with different values of the parameters listed in Table 2 have shown a well-defined dependence only with respect to the bending elastic modulus $\kappa$ for a given temperature. As a matter of fact, ELDOR observables are found to be independent of the effective lateral tension $\sigma$, of the viscosity of the surrounding fluid $\eta$, and of the size of the vesicle $R_0$, (this is strictly true for $R_0 > 100$ nm). This is an important conclusion, which simplifies to a large extent the analysis of the experimental data because only one physical parameter has to be determined. Furthermore, such a conclusion can be justified by considering that, with the physical parameters in the same range as those in Table 2, the following approximation can be employed for the director

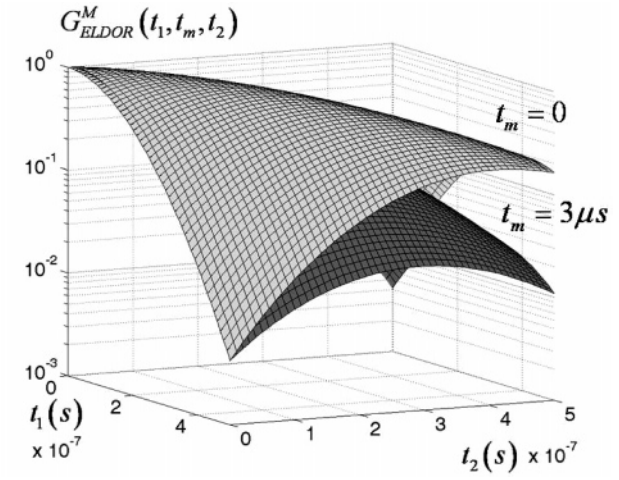


**Figure 11.** Time dependence of the characteristic function $G^M_{ELDOR}(t_1,t_m,t_2)$ of the 2D-ELDOR experiment describing the director fluctuation contribution of a nitroxide spin probe in quasi- spherical vesicles. The time profiles refer to two different values of the mixing time, i.e., $t_m = 0$ (upper surface) and $t_m = 3$ $\mu$s (lower surface). The parameter values used in the calculation are listed in Table 2, the employed magnetic anisotropy is $(\delta\omega'_M)^2 = 5.8 \times 10^{15}$ s$^{-2}$.

correlation function,

$$\overline{n_x(0)n_x(t)} = \frac{k_BT}{12\pi\kappa}\ln(t_b/t) \qquad (81)$$

where $\eta$, $R_0$, and $\sigma$ enter only through the parameter $t_b$. In Appendix A, we have reported the analysis leading to such an approximation. Interestingly, the use of eq 81 leads to time integrals for the functions $g(t)$ and $g_{1,2}(t_1, t_m, t_2)$, which can be performed analytically. Thus, one obtains as the characteristic function of the ELDOR experiment

$$\ln\{G^M_{ELDOR}(t, t_m, t)\} = -(\delta\omega_M')^2\frac{k_BT}{12\pi\kappa}\Big[-t^2\Big(\ln t - \frac{3}{2}\Big) + (2t+t_m)^2\Big(\frac{1}{2}\ln(2t+t_m) - \frac{3}{4}\Big) - (t+t_m)^2\Big(\ln(2t+t_m) - \frac{3}{2}\Big) + t_m^2\Big(\frac{1}{2}\ln t_m - \frac{3}{4}\Big)\Big] \qquad (82)$$

where all the terms containing $t_b$ (see eq A-5) cancel out exactly, thereby explaining the independence of the ELDOR signal with respect to the $\eta$, $R_0$, and $\sigma$ parameters. Althoug eq 82 represents the easiest way to evaluate the ELDOR relaxation time, in the following, we shall report the results with the full correlation function to avoid any possible deviation from the approximate form, eq 81.

In summary, the bending elastic modulus $\kappa$ is, apart from the strength of the magnetic interactions, the relevant parameter determining the transverse relaxation time at a given temperature. Figure 12 shows the decay profile along the $t_1 = t_2 = t$ direction of the function $G^M_{ELDOR}(t_1, t_m, t_2)$ for two different values of the bending elastic modulus: increasing this parameter entails a slower decay of the signal. Indeed, a stiffening of the vesicles determines a reduction of the amplitude of the shape fluctuations and a faster decay of reorientational correlations. Clearly, the bending elastic modulus is also the crucial parameter in determining the variation of the transverse relaxation rates $(T^M_{2,DF})^{-1}$ with the mixing time $t_m$. This is shown in Figure 13 for five different values of the bending elastic modulus $\kappa$. For simplicity, the molecular tumbling contribution was set to zero, i.e., $(T^M_{2,mol})^{-1} = 0$. One sees that

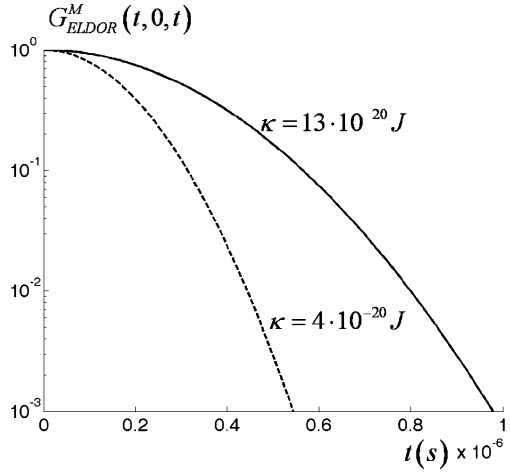


**Figure 12.** Time dependence of the characteristic function $G^{M}_{ELDOR}(t,0,t)$ of the 2D-ELDOR experiment calculated for $t_1 = t_2 = t$ and a vanishing mixing time, $t_m = 0$. The time profiles refer to two different values of the bending elastic modulus $\kappa$ of the vesicle, i.e., $\kappa = 4 \times 10^{-20}$ J (dashed line) and $\kappa = 13 \times 10^{-20}$ J (continuous line). The parameter values used in the calculation are listed in Table 2, the employed magnetic anisotropy is $(\delta\omega'_M)^2 = 5.8 \times 10^{15}$ s$^{-2}$.

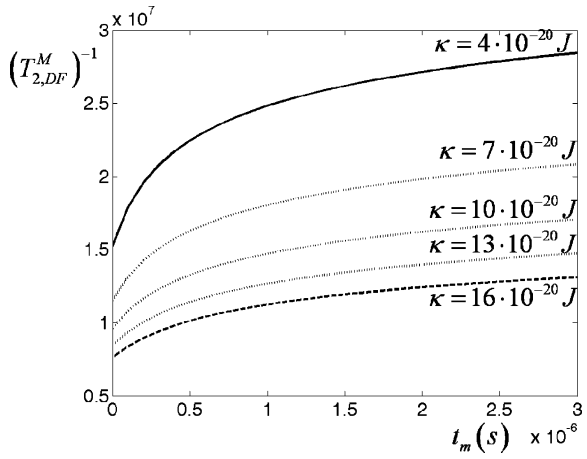


**Figure 13.** Dependence of the transverse relaxation rate $(T^{M}_{2,DF})^{-1}$, arising from vesicle shape fluctuations, on the mixing time $t_m$ in a 2D-ELDOR experiment. The calculations refer to five different values of the bending elastic modulus $\kappa$ and a vanishing molecular tumbling contribution, $(T^{M}_{2,mol})^{-1} = 0$. The other parameter values are listed in Table 2, the employed magnetic anisotropy is $(\delta\omega'_M)^2 = 5.8 \times 10^{15}$ s$^{-2}$.

as long as a time window of microseconds is accessible for $t_m$, the bending elastic modulus can be determined from this type of ELDOR experiments.

**Microscopic Order/Macroscopic Disorder (MOMD) Effect.** Actually, the experimental ESR spectrum of a vesicle sample is a superposition of spectra from locally ordered environments (or fragments), which are randomly distributed with respect to the direction of the constant magnetic field, i.e., the lab **Z** axis. As long as the lateral diffusion of the spin probe molecules is slow compare to the time scale of the experiment, the measured ESR signal can be written as

$$S_{c^-}^{MOMD} = \int S_{c^-}(\theta_B) \sin \theta_B \, d\theta_B \qquad (83)$$

where $S_{c^-}(\theta_B)$ is the ESR spectrum of a particular membrane fragment characterized by the angle $\theta_B$ between the bilayer normal (**z**-axis of the average director frame) and the magnetic field.

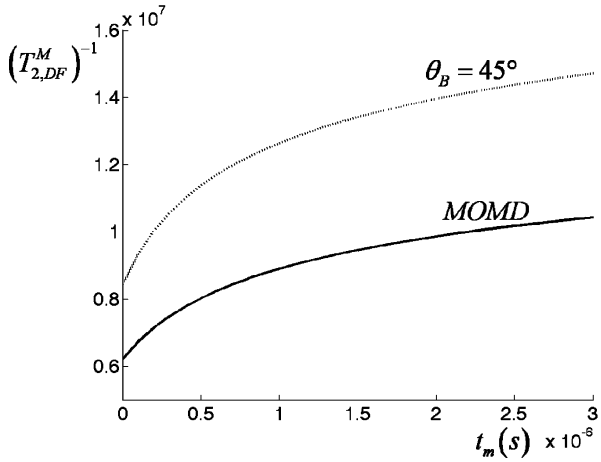


**Figure 14.** Dependence of the transverse relaxation rate $(T^{M}_{2,DF})^{-1}$, arising from vesicle shape fluctuations, on the mixing time $t_m$ in a 2D-ELDOR experiment. The two relaxation curves refer to a particular orientation $\theta_B = \pi/4$ (dotted line) of the average director and magnetic field and to the MOMD (microscopic order/macroscopic disorder) average (solid line). The other parameter values are listed in Table 2, the employed magnetic anisotropy is $(\delta\omega'_M)^2 = 5.8 \times 10^{15}$ s$^{-2}$.

The MOMD case is important for biologically relevant membrane systems, where it is not easily possible to prepare macroscopically aligned samples, but macroscopically disordered "dispersion" samples are readily available. Now, let us examine the MOMD effects on the contribution of the director fluctuations to the relaxation. First, we note that, because of the "echo-like" cancellation of the inhomogeneous broadening along the temporal dimension, $t_1 = t_2$, the different orientations of the ADF with respect the LF do not induce any change in the resonance frequency of the resulting line shape. On the other hand, the variations of the coefficients $\delta\omega'_M(\theta_B)$ have to be considered according to Figure 9. Clearly, the dependence of the line width on the angle $\theta_B$ follows the behavior of the coefficient $\delta\omega'_M(\theta_B)$: when it is near its maximum value, the corresponding membrane regions give a broader absorption, while those for which $\delta\omega'_M(\theta_B)$ is small contribute with a narrower signal. The resulting line shape is calculated according to eq 83.

In addition, the dependence of the ELDOR line width on the mixing time $t_m$ is affected by MOMD, as shown in Figure 14. One sees that both the absolute value of $(T^{M}_{2,DF})^{-1}$ as well as the variation of $(T^{M}_{2,DF})^{-1}$ with $t_m$ are attenuated but the overall behavior of $(T^{M}_{2,DF})^{-1}$ is unchanged. This indicates that 2D-ELDOR studies of macroscopically disordered samples still allow a reliable characterization of director fluctuations.

**Analysis of the Experimental Data.** In this section, the experimental results obtained by Patyal at al.[20] are interpreted in terms of the relaxation model developed in this paper. However, the study of the transverse relaxation rates as a function of the mixing time was not the principal aim of the experimental ELDOR study, so only limited results are available for an analysis of the collective motions. Nevertheless, it can be shown that the model calculations are in good agreement with the experimental observations, and reasonable values for the bending elastic modulus $\kappa$ of the DPPC vesicles can be extracted from the analysis of the data. As we have extensively discussed in the previous sections, two parameters are relevant in order to fully characterize the mixing time dependence of the transverse relaxation rates in an ELDOR experiment of a vesicle sample: the bending elastic modulus $\kappa$ and the molecular contribution $T^{M}_{2,mol}$ to the relaxation. In Figures 15 and 16, the

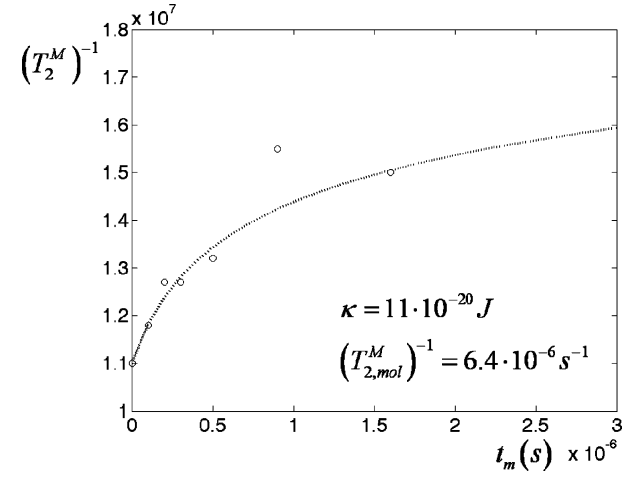


**Figure 15.** Dependence of the transverse relaxation rate $(T_2^{\mathrm{M}})^{-1}$ on the mixing time $t_{\mathrm{m}}$ in a 2D-ELDOR experiment for pure DPPC vesicles at 45 °C. Experimental data taken from ref 20 are indicated by open circles. The dotted line represents a best-fit simulation based on the slow-motional model developed in this paper. The fit parameters are $\kappa = 11 \times 10^{-20}$ J and $(T_{2,\mathrm{mol}}^{\mathrm{M}})^{-1} = 6.4 \times 10^{6}$ s$^{-1}$.

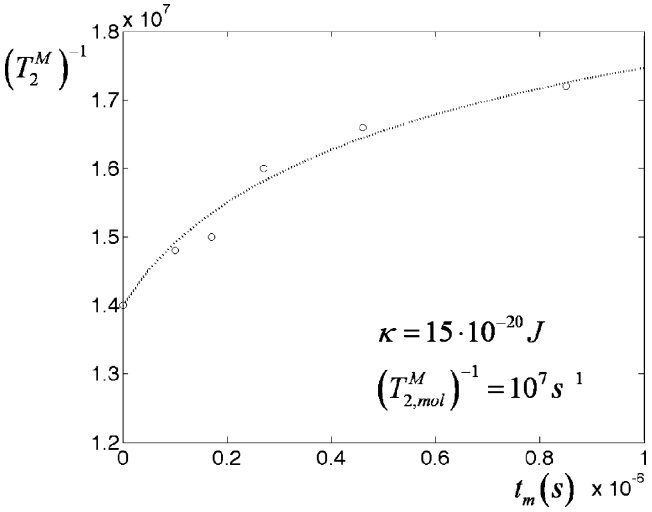


**Figure 16.** Dependence of the transverse relaxation rate $(T_2^{\mathrm{M}})^{-1}$ on the mixing time $t_{\mathrm{m}}$ in a 2D-ELDOR experiment for mixed DPPC/GA vesicles (molar ratio 5:1) at 45 °C. Experimental data taken from ref 20 are indicated by open circles. The dotted line represents a best-fit simulation based on the slow-motional model developed in this paper. The fit parameters are $\kappa = 15 \times 10^{-20}$ J and $(T_{2,\mathrm{mol}}^{\mathrm{M}})^{-1} = 1 \times 10^{7}$ s$^{-1}$.

transverse relaxation rates $(T_2^M)^{-1}$ of the ELDOR experiments are plotted as a function of the mixing time $t_{\mathrm{m}}$. Results are shown for pure DPPC vesicles (Figure 15) and for DPPC/GA mixed vesicles (molar ratio 5:1) (Figure 16), respectively. In each case, the experimental data (open circles) refer to the $M = 1$ hyperfine line and a temperature of 45 °C. One observes a pronounced dependence of the relaxation rate $(T_2^M)^{-1}$ on the mixing time $t_{\mathrm{m}}$, indicating that director fluctuations constitute the dominant relaxation process. Consequently, we can analyze the relaxation curves on the basis of the relaxation model developed in this paper. The employed magnetic parameters of the spin probe are summarized in Table 1. Calculated relaxation curves were fitted to the experimental curves by varying the parameters $\kappa$ and $(T_{2,\mathrm{mol}}^M)^{-1}$. In the calculations, the MOMD effect has been considered. The resulting values of $\kappa$ and $(T_{2,\mathrm{mol}}^M)^{-1}$ parameters are reported in Table 3. The dotted lines in Figures 15 and 16 represent the best simulations of the relaxation curves. Evidently, the agreement between experiment and theory is good.

**TABLE 3: Bending Elastic Moduli and Transverse Molecular Relaxation Rates Extracted from 2D-ELDOR Experiments[a] Using a Slow-Motional Model**

| sample | temp (°C) | $\kappa$ (J) | $(T_{2,\mathrm{mol}}^{\mathrm{M}})^{-1}$ ($10^6$ s$^{-1}$) |
|---|---|---|---|
| DPPC[b] | 45 | $11 \times 10^{-20}$ | 6.4 |
| DPPC | 70 | $4.7 \times 10^{-20}$ | 4.4 |
| DPPC/GA[c] | 45 | $15 \times 10^{-20}$ | 10 |
| DPPC/GA | 70 | $8 \times 10^{-20}$ | 6.6 |

[a] Experimental data adopted from ref 20. [b] DPPC: (1,2-dipalmitoyl-*sn*-glycero-phosphatidylcholine). [c] GA: gramicidin A′.

Several experimental techniques have been developed in order to quantitatively study the bending rigidity of vesicles and its temperature dependence: our result of $\kappa = 11 \times 10^{-20}$ J for pure DPPC vesicles at 45 °C compares favorably with those obtained by heat capacity measurements,[38] video microscopy[39] and optical techniques.[40] It should also be mentioned that the bending moduli of fluid-phase phosphatidylcholine (PC) membranes, which have been determined by NMR,[43] are substantially smaller than that for DPPC. In our case, however, the spin probe 16-PC given its low concentration, contributes only slightly to the elastic properties of the system, and the bending modulus can be identified with that of pure DPPC. For DPPC/GA mixed vesicles at 45 °C, a value of $\kappa = 15 \times 10^{-20}$ J is estimated in the present study. Evidently, gramicidin (a membrane peptide) causes a stiffening of the vesicles, increasing the bending elastic modulus significantly.[15,41] Inspection of Table 3 reveals that the value of $\kappa$ sensitively depends on the temperature of the sample. Notably, $\kappa$ decreases by a factor of 2 when the temperature is raised from 45 °C to 70 °C. This is in agreement with previous results for other phospholipid vesicles.[15]

In summary, the values for $\kappa$ are reasonable and indicate that transverse electron spin relaxation is able to provide information concerning viscoelastic properties in biological membranes.

## Conclusion

An analytical theory for the dependence of the transverse relaxation times for the auto-peaks in 2D-ELDOR experiments on membrane vesicles has been developed. It is based upon treating fluctuations of the director field as a multidimensional Gaussian process, and it includes just the secular contributions of the fluctuating part of the spin Hamiltonian. The main outcome of this theoretical analysis is that the time-dependent ELDOR signal, which can be used to define the transverse relaxation time, is specified in terms of the correlation function describing the director fluctuations at the spin probe location. Moreover, it is shown that the transverse relaxation time displays a definite dependence on the mixing time $t_{\mathrm{m}}$ whenever some dynamical process, which modulates the magnetic interaction, occurs in a comparable time scale. Our theory provides precise tools for the interpretation of the 2D-ELDOR experiments of ordered fluids once the correlation function for the director fluctuations is evaluated according to standard viscoelastic models for collective fluctuations of the systems considered.

In the present analysis, the model for the shape fluctuations of quasispherical vesicles has been considered in detail, and good agreement has been found in the comparison with experiments. The theory provides a useful way to extract $\kappa$, the bending elastic modulus of the membranes, from experiments. Of particular importance from a biological point of view is that the technique may be exploited to investigate modifications of membrane viscoelastic behavior caused by inclusion of sterols, peptides, or proteins. Indeed, these effects are not small and invite speculation regarding the consequences for overall biological membrane functions.

Finally, we recall that the present theory is confined to the diagonal peaks of the ELDOR spectra because of the secular approximation invoked in the analysis. According to a previous treatment of CW-ESR spectra,[18] we expect a negligible contribution to the autopeaks due to the fluctuating pseudosecular contribution of the hyperfine interactions, while they should have a major role in determining the shape of the cross-peaks. Theoretical work is in progress in order to extend the theory to account for the fluctuating pseudosecular terms of the spin Hamiltonian.

**Acknowledgment.** This work was supported by the Italian Ministry for Universities and Scientific Research, through a project PRIN. This work was also supported by National Institutes of Health grants P41RR16292 and EB03150 (J.H.F.).

## Appendix A: Approximate Form of the Correlation Function $\overline{n_x(0)n_x(t)}$ for Quasispherical Fluctuations of Membrane Vesicles

By scaling the time according to the parameter

$$t_s = \frac{4\eta R_0^{\,3}}{\kappa} \tag{A-1}$$

the correlation function of the director fluctuation, eq 81, is conveniently represented as

$$\overline{n_x(0)n_x(t)} = \frac{k_B T}{12\pi\kappa} f(\hat{t}) \tag{A-2}$$

where $\hat{t}$ is the scaled time, $\hat{t} = t/t_s$, and the function $f(\hat{t})$

$$f(\hat{t}) = \sum_{l=2}^{l_{max}} 3b_l\, e^{-\hat{t}a_l} \tag{A-3}$$

is specified through the coefficients

$$a_l = \frac{4}{\hat{\tau}_l} = \frac{4(l-1)l(l+1)(l+2)(l^2+l+\sigma)}{(2l+1)(2l^2+2l-1)}$$

$$b_l = \frac{l(l+1)(2l+1)}{2(l+2)(l-1)(l^2+l+\sigma)} \tag{A-4}$$

We stress that the function $f(\hat{t})$ depends on the physical parameters describing the vesicle system only through $\sigma$ and $l_{max}$. In Figure 17, we have represented the profile of such a function for two values of $l_{max}$ and two values of $\sigma$ by employing a logarithmic scale for the time axis. Some key features are clearly evident: (i) the function is initially constant, with the value $f(0)$ depending on $l_{max}$ and $\sigma$; (ii) at intermediate time, $f(\hat{t})$ displays a linear dependence on $\ln(\hat{t})$ and is a function of the surface tension $\sigma$ which determines a shift in the values. The linear regime ends up with the final relaxation with very small values of such a function. Once one fixes the value of $\sigma$, the scaled correlation function acquires a universal character in the time window of the linear dependence, so that one can employ the following representation for the linear behavior

$$f(\hat{t}) = \ln(\hat{t}_b/\hat{t}) \tag{A-5}$$

with the parameter $\hat{t}_b$ dependent on the $\sigma$ value. The particular value of such a parameter has to be optimized by fitting the linear portion of the profiles in Figure 17. For instance, the value $\hat{t}_b = 0.1901$ has been obtained for the case $\sigma = 0$. Then, given

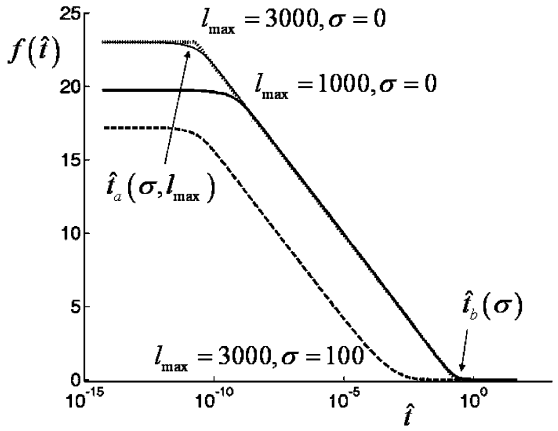


**Figure 17.** Representation of the scaled correlation function $f(\hat{t})$ for two values of $l_{max}$ and two values of $\sigma$: dashed line ($l_{max} = 3000$, $\sigma = 100$), heavy continuous line ($l_{max} = 1000$, $\sigma = 0$), light continuous line ($l_{max} = 3000$, $\sigma = 0$). For the latter case, the approximate form is also depicted (dotted lines).

$f(0)$, evaluated according to eq A-3, the following approximation is derived for the function in the entire time domains

$$f(\hat{t}) = \begin{cases} f(0) & \text{for } \hat{t} \le \hat{t}_a \\ \ln(\hat{t}_b/\hat{t}) & \text{for } \hat{t}_a \le \hat{t} \le \hat{t}_b \\ 0 & \text{for } \hat{t} \ge \hat{t}_b \end{cases} \tag{A-6}$$

with a further parameter $\hat{t}_a$, dependent on $l_{max}$ and $\sigma$, to be obtained by matching the linear behavior with the initial value of the function

$$\ln \hat{t}_a = \ln \hat{t}_b - f(0) \tag{A-7}$$

For the sake of comparison, in Figure 17, we have also represented the approximation eq A-6 for $\sigma = 0$, and a very good agreement is recovered, particularly in the linear regime. It should be mentioned that approximation eq A-6 can be justified under the assumption of a vanishing lateral tension on the basis of an integral representation for the summation in eq A-3. Indeed, for the coefficients eq A-4, the following limiting behavior is found for large $l$

$$b_l \sim \frac{1}{l} \quad a_l \sim l^3 \tag{A-8}$$

which can be exploited to convert the summation of eq A-3 into the integral form

$$f(\hat{t}) = 3\int_{x_0}^{x_{max}} dx \frac{e^{-\hat{t}x^3}}{x} \tag{A-9}$$

where the boundaries $x_0$ and $x_{max}$ are adjustable parameters required to achieve the numerical matching between eqs A-3 and A-9. By performing the change of variables $x \rightarrow y = x^3\hat{t}$, one obtains

$$f(\hat{t}) = \int_{x_0{}^3\hat{t}}^{x_{max}{}^3\hat{t}} dy \frac{e^{-y}}{y} = E_1(x_0{}^3\hat{t}) - E_1(x_{max}{}^3\hat{t}) \tag{A-10}$$

where $E_1(z)$ denotes the "exponential integral" function[42]

$$E_1(z) = \int_z^{\infty} du \frac{e^{-u}}{u} \tag{A-11}$$

having the asymptotic limits $E_1(z) \cong 0$ for $z \gg 1$ and $E_1(z) \cong -\ln\gamma - \ln z$ for $z \ll 1$, where $\gamma$ is the Euler number. Then, in

agreement with eq A-6, a vanishing value and a constant value are recovered for $\hat{t} \gg 1/x_0^3$ and for $\hat{t} \ll 1/x_{max}^3$, respectively, while a linear behavior eq A-5 is found for $1/x_{max}^3 \ll \hat{t} \ll 1/x_0^3$.

In summary, the behavior of $f(\hat{t})$ can be specified through the scaled parameters $\hat{t}_a$ and $\hat{t}_b$, which, once converted to real time units by accounting for $t_s$ in eq A-1, take on typical values of a fraction of picoseconds and a few milliseconds by using representative parameters of Table 2 for a vesicle system. Thus, in the time scale of microseconds characterizing the mixing time in the ELDOR experiments, we are allowed to use the linear approximation eq A-5. Correspondingly, the correlation function for the director fluctuations in quasispherical vesicles can be represented as

$$\overline{n_x(0)n_x(t)} = \frac{k_B T}{12\pi\kappa} \ln(\hat{t}_b/\hat{t}) = \frac{k_B T}{12\pi\kappa} \ln(t_b/t) \quad \text{(A-12)}$$

where $t_b = t_s\hat{t}_b$.

## References and Notes


(1) Redfield, A. G. *Adv. Magn. Reson.* **1965**, *1*, 1.
(2) Freed, J. H.; Fraenkel, G. K. *J. Chem. Phys.* **1963**, *39*, 326−348.
(3) Kubo, R. *J. Math. Phys*. **1963**, *4*, 174.
(4) Kubo, R.; Toda, M.; Hashitsume, N. *Statistical Physics II*; Springer-Verlag: Berlin, 1985.
(5) Freed, J. H.; Bruno, G. V.; Polnaszek C. F. *J. Phys. Chem.* **1971**, *75*, 3385−3399.
(6) Polnaszek, C. F.; Bruno, G. V.; Freed, J. H. *J. Chem. Phys.* **1973**, *58*, 3185.
(7) Freed, J. H. In *Spin Labeling: Theory and Applications;* Berliner, L. J., Ed.; Academic: New York, 1976.
(8) Moro, G.; Freed, J. H. *J. Chem. Phys.* **1981**, *74*, 3757.
(9) Groupe d′Etude des Cristaux Liquides (Orsay), *J. Chem. Phys.* **1969**, *51*, 2.
(10) de Gennes, P. G. *The Physics of Liquid Crystal*, Clarendon: Oxford, 1974.
(11) Freed, J. H. *J. Chem. Phys.* **1977**, *66*, 4183.
(12) The analysis of director fluctuations in case of slow molecular motions, besides being extremely difficult, is only of secondary interest because director fluctuations produce changes in the resonance frequencies that are much smaller than those arising from the wide angle rotations of the probe. Correspondingly, we expect that fluctuations of resonance frequencies are mainly controlled by the probe molecules tumbling in the rotational slow motion regime. The fast tumbling regime is the most favourable situation for observation of director fluctuations in the ESR observables.
(13) Frezzato, D.; Kothe, G.; Moro, G. J. *J. Phys. Chem. B* **2001**, *105*, 1281.
(14) Althoff, G.; Frezzato, D.; Vilfan, M.; Stauch, O.; Schubert, R.; Vilfan, I.; Moro, G. J.; Kothe, G. *J. Phys. Chem. B* **2002**, *106*, 5506.
(15) Althoff, G.; Stauch, O.; Vilfan, M.; Frezzato, D.; Moro, G. J.; Hauser, P.; Schubert, R.; Kothe, G. *J. Phys. Chem. B* **2002**, *106*, 5517.
(16) Frezzato, D.; Moro, G. J.; M. Tittelbach, Kothe, G. *J. Chem. Phys.* **2003**, *119*, 4060.
(17) Frezzato, D.; Moro, G. J.; Kothe, G. *J. Chem. Phys.* **2003**, *119*, 6931; Frezzato, D.; Kothe, G.; Moro, G. J. *J. Chem. Phys.* **2003**, *119*, 6946.
(18) Frezzato, D.; Kothe, G.; Moro, G. J. *J. Phys. Chem. B* **2004**, *108*, 9505.
(19) Lee, S.; Budil, D.; Freed, J. H. *J. Chem. Phys.* **1994**, *101*, 5529.
(20) Patyal, B.; Crepeau, R.; Freed, J. H. *Biophys. J.* **1997**, *73*, 2201.
(21) Crepeau, R.; Saxena, S.; Lee, S.; Patyal, B.; Freed, J. H. *Biophys. J.* **1994**, *66*, 1489.
(22) Lee, S.; Patyal, B.; Saxena, S.; Crepeau, R.; Freed, J. H. *Chem. Phys. Lett.* **1994**, *221*, 397.
(23) Gardiner, C. W. *Handbook of Stochastic Methods*; Springer-Verlag: Berlin, 1983.
(24) Gorcester, J.; Freed, J. H. *J. Chem. Phys.* **1988**, *88*, 4678.
(25) Liang Z.; Freed J. H. *J. Magn. Reson.* **2005**, *177*, 247−260.
(26) Slichter, C. P. In *Principles of Magnetic Resonance*; Harper: New York, 1964.
(27) Gamliel, D.; Freed, J. H. *J. Magn. Reson.* **1990**, *89*, 60.
(28) Lipowsky, R., Sackmann, E., Eds. *Structure and Dynamics of Membranes*; Elsevier: Amsterdam, 1995.
(29) Halle, B. *Phys. Rev. E* **1994**, *50*, R2415.
(30) Halle, B.; Gustafsson, S. *Phys. Rev. E* **1997**, *56*, 690.
(31) Lasic, D. D. *Biochem. J.* **1988**, *256*, 1−11.
(32) Niggemann, G., Kummrow, M., Helfrich, W. *J. Phys. II* **1995**, *5*, 413−425.
(33) Nordio, P. L.; Busolin, P. *J. Chem. Phys.* **1971**, *55*, 5485.
(34) Milner, S. T.; Safran, S. A. *Phys. Rev. A* **1987**, *36*, 4371.
(35) Helfrich, W. *Z. Naturforsch.* **1973**, *28*, 693.
(36) Schneider, M. B.; Jenkins, J. T.; Webb, W. W. *J. Phys.* **1984**, *45*, 1457.
(37) Hackl, W.; Seifert, U.; Sackmann, E. *J. Phys. II* **1987**, *7*, 1141.
(38) T. Heimburg, *Biochim. Biophys. Acta* **1998**, *147*, 1415.
(39) Fernandez-Puente, L.; Bivas, I.; Mitov, M. D.; Meleard, P. *Europhys. Lett.* **1994**, *28*, 181.
(40) Lee, C.-H.; Lin, W.-C.; Wang, J. *Phys. Rev. E* **200**1, *64*, 020901-(R).
(41) Chen, C. M. *Physica A* **2000**, *281*, 41−50.
(42) Abramowitz, M.; Stegun, I. A. *Handbook of Mathematical Functions*; Courier Dover: New York, 1965; p 229, eq 5.1.11.
(43) Martinez, G. V.; Dykstra, E. M.; Lope-Piedrafita, S.; Job, C.; Brown, M. F. *Phys. Rev. E* **2002**, *66*, 050902(R).